EUROPEAN COMMISSION

Community Research

SEVENTH FRAMEWORK PROGRAMME

ARCHER

Collaborative Project (CP)

Co-funded by the European Commission under the Euratom Research and Training Programme on Nuclear Energy within the Seventh Framework Programme

Grant Agreement Number : 269892

Start date : 01/02/2011 Duration : 48 Months
www.archer-project.eu

Archer
Advanced Reactor for Cogeneration of Heat & Electricity-R&D

Characteristic Dust Parameters, depending on Graphite Grade and Friction Forces

Authors : Max Schreier, Martin Lustfeld,
Wolfgang Lippmann, Antonio Hurtado (all TUD)

ARCHER - Contract Number: 269892
Advanced High-Temperature Reactors for Cogeneration of Heat and Electricity R&D
EC Scientific Officer: Dr. Panagiotis Manolatos

Document title	Characteristic Dust Parameters, depending on Graphite Grade and Friction Forces
Author(s)	Max Schreier, Martin Lustfeld, Wolfgang Lippmann, Antonio Hurtado (all TUD)
Number of pages	49
Document type	Deliverable
Work Package	WP 23
Document number	D23.23
Issued by	TU Dresden
Date of completion	26/11/2014
Dissemination level	Confidential, only for members of the consortium (including the Commission Services).

Summary

Graphite dust generation due to the abrasion of graphite core material is a significant safety issue in Pebble Bed High Temperature Reactors. Objective of this task is to establish a small-scale experimental facility producing dust particles under conditions as close as possible to those existing in a reactor pebble bed. Experiments were performed with test facility "Pebble Mill" and graphite dust was generated under different load scenarios. Analysis of the particles was performed using laser scanning microscopy and the image processing tool ImageJ. The results of these analyses are described in the paper.

Approval

Date	By
03/12/2014	Karl VERFONDERN
15/01/2015	Norbert KOHTZ
15/01/2015	Steven KNOL

Distribution list

Name	Organisation	Comments
P. Manolatos	EC DG RTD	Through the EC participant portal
All beneficiaries	ARCHER	Through the private online workspace

1 Introduction

Graphite dust production in the primary circuit is a significant safety issue in High Temperature Reactors, particular in the pebble bed configuration [1]. In case of a Depressurized Loss of Forced Coolant accident (DLOFC), radioactively contaminated graphite dust can be remobilized from the deposition sites and blown out of the primary circuit and even the reactor system boundaries. This would contribute to the radioactive source term of such an accident possibly above legal limits. Additionally, graphite dust deposition on primary circuit components such as heat exchangers can lead to a degradation of their performance. Therefore, thorough simulations of the graphite dust transport in HTR primary circuits are carried out by numerous research groups in order to determine the amount of radioactively contaminated dust that can be remobilized under accident conditions [2]. Based on these results, retention systems for dust particles can be designed.

A major unknown when performing such analyses are the characteristics of the graphite particles themselves. Even though considerable quantities of graphite particles were found both in the experimental reactor AVR and in the prototype reactor THTR-300, they do not allow a generalization for graphite dust characteristics in the primary circuit of other HTR systems. This is primarily due to incidents that occurred in AVR and THTR, but are unlikely to happen in modern HTR systems such as ingress of large amounts of impurities into the primary circuit or the rupture of a significant number of fuel pebbles.

1.1 Particle analysis methodology

For optical evaluation of the particles a 3D laser scanning microscope with a maximum optical magnification of 150x yielding image files with a resolution of 1024x768 was used. Particles are broadly distributed in size, and their shape in general is complex and very different from an ideal sphere [3]. Therefore, adequate particle characterization not only needs to take into account the particle size distribution, but also a measure of their shape.

Analyses of particle images obtained from the laser microscope were carried out using digital image processing. As Image processing tool, the software ImageJ was chosen due to its very high variability and adaptability, as well as its wide recognition in the field of image processing. It is a freely available, platform-independent tool developed by Wayne Rasband from U.S. National Institutes of Health. It is widely applied in the field of micrograph analyses [4]. The general approach to particle analysis using this image processing tool is schematically represented in Figure 1.

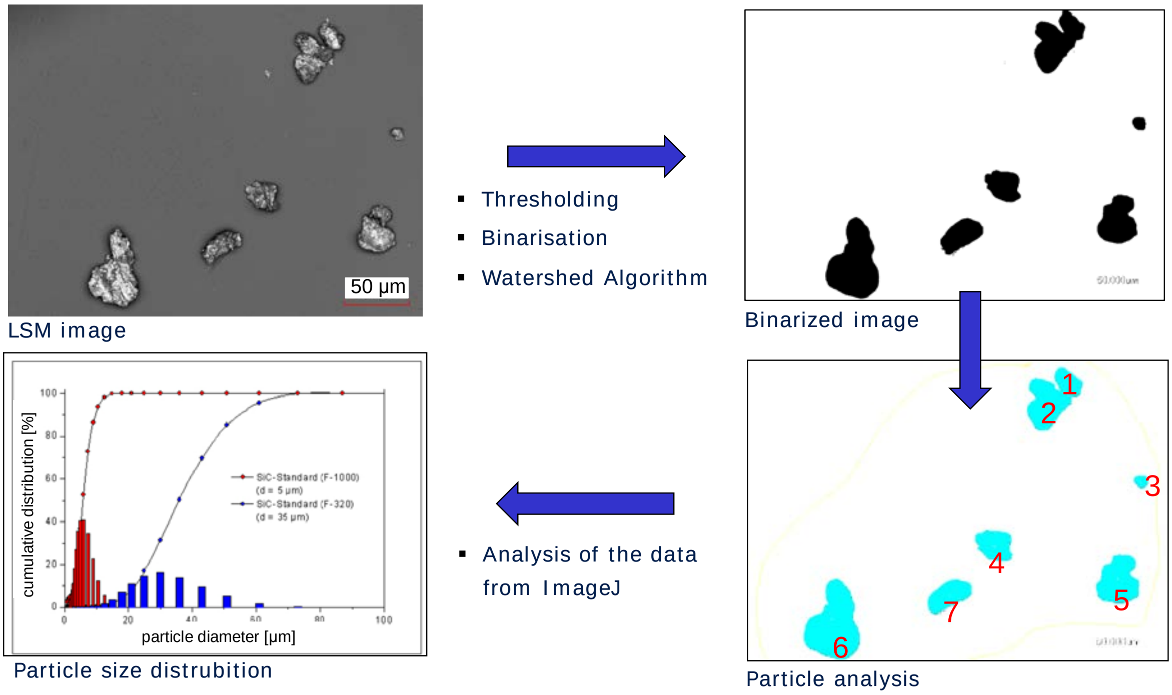

Figure 1: Image processing procedure using the ImageJ software package [3]

In the first step, the images are converted from greyscale into black/white binary image files in order to perform the particle analysis algorithm available in ImageJ. To achieve the best possible result, the threshold shade of grey that belongs to the particle image (as opposed to the background) needs to be identified individually for each image. After this procedure, the binary images are converted to matrixes of black pixels and coherent areas of pixels are recognized as the projected areas of the original particles. In the subsequent analyses, the number of pixels contained in each area representing a particle are counted and converted into an equivalent particle surface size which is calculated based on a fixed relation of µm² per pixel. The thereby determined particles are saved in a data sheet along with their respective sizes. Further analyses can be performed with conventional spreadsheet processors such as MS Excel or Matlab.

1.2 Determination of the particle size distribution

Here, the projected surface size is used as a basis to calculate equivalent particle diameters (Figure 2) which can be statistically evaluated to yield a particle size distribution.

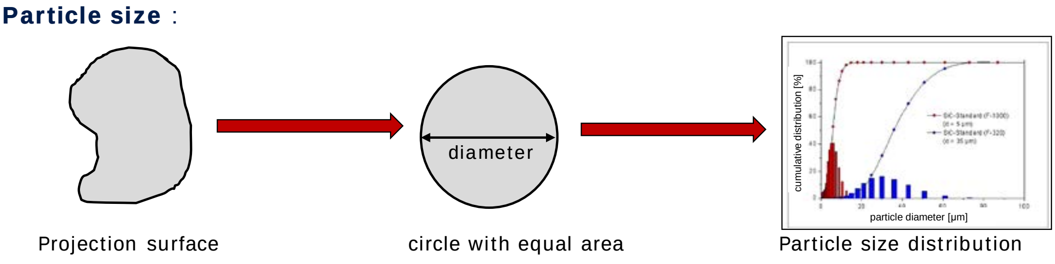

Figure 2: Calculation of equivalent particle diameters based on particle data available from evaluation with the ImageJ tool

In order to facilitate further analyses, if non-spherical particles are to be characterized as in this case, an equivalent particle diameter can be defined, which allows treatment of these non-spherical particles as spherical particles up to a certain extent. In this work, commonly used particle size spectrometers could not be used due to the limited amount of generated graphite powder. Based on the laser scanning microscope images, the equivalent diameter here is simply defined as the diameter of a circle that exhibits the same area as the 2-dimensional projection of the particle under investigation (Figure 2). At this point, the third dimension is not taken into account. However, since measurement of the particle height is possible, the methodology could be extended to consider the particle volume as well and compare it to the volume of a sphere. Given a sufficient amount of particles analyzed (N>2000), the particle collectivity can be evaluated statistically yielding a particle size distribution (PSD). The PSD is characteristic for the collectivity of graphite particles under consideration and depends on all experimental parameters such as the graphite grade and the load applied during abrasion. Major parameters of the PSD allowing comparison of different particle species are the mean particle diameter đ and the median particle diameter d_{50}. The median particle diameter is defined as the particle diameter value for which 50% of the particles are smaller and the other 50% are larger.
In general, the comparability of particle sizes measured using different definitions for equivalent diameters need to be cautiously considered. Using such equivalent particle diameters as an input for computational fluid dynamics simulations is problematic as well, since the information on particle shape is not taken into account. Notably, secondary motion for non-spherical and in particular for disc-shaped graphite particles can be significant and must therefore not be excluded from the overall analysis. Characterization of the particle shape is further discussed in the following section.

1.3 Characterization of the particle shape

A simple way to systematically characterize the particle shape is determining its aspect ratio, the ratio between length and width of a particle. In this work, the aspect ratio is determined based on the shape of the projected particles described in the previous section. The Feret diameter, on which all further analysis is based, is defined as the length of a straight line from one side of the 2-dimensional particle image to the other side [5]. For non-circular particles, this results in different Feret diameters for different angles in which the straight line is marked on the particle. Therefore, there are two distinct angles for which the Feret diameters attain a minimum and a maximum value. These minimum and maximum Feret diameters are determined for each particle in order to calculate the aspect ratio after the following formula.

$$aspect\ ratio = \frac{minimum\ Feret\ diameter}{maximum\ Feret\ diameter} = \frac{x_{Fe\_min}}{x_{Fe\_max}} \quad (1)$$

The principle for determining both the minimum and the maximum Feret diameters is illustrated in Figure 3.

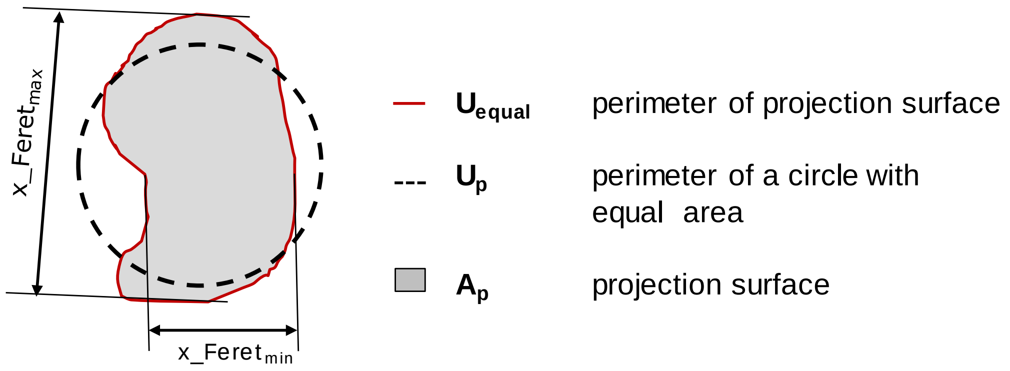

Figure 3: Determination of shape factors based on the projected area of graphite particles [3]

Thus, in case of spherical particles, the aspect ratio is 1, whereas it tends to 0 for very long, rod-shaped particles.

A further parameter to characterize the particle shape is its sphericity (for 3-dimensional images). For the images considered here, the 2-dimensional equivalent is the circularity Ψ of a particle defined after the following formula.

$$\Psi = \frac{circumference\ of\ a\ sphere\ with\ equivalent\ area}{circumference\ of\ the\ 2-dimensional\ particle\ image}$$

For perfectly circular particles, this definition yields a value of Ψ=1, while for any other shape a value Ψ≤1 is obtained, since the circumference of an arbitrarily shaped geometry is always larger than that of a circle with the same area. Based on the projected area A_p obtained using the ImageJ tool as described above, the following formula applies to determine the circularity:

$$\Psi = \frac{U_{equal}}{U_p} = \frac{2 \cdot \sqrt{\pi \cdot A_p}}{U_p} \qquad with\ U_{equal} = 2 \cdot \pi \cdot \sqrt{\frac{A_p}{\pi}} = 2 \cdot \sqrt{\pi \cdot A_p} \qquad (2)$$

Aspect ratio and circularity aren't bijective, which means that knowing the aspect ratio is not sufficient to specify the circularity and vice versa. However, the aspect ratio is a value which can easily be statistically evaluated and which gives basic information on to which extent particles deviate from the perfect circular or spherical shape. Literature on simulation of non-spherical particles gives a value for the aspect ratio of at least 0.6 for which particles can be treated as spherical particles, neglecting their secondary motion. However, at lower values of the aspect ratio, the secondary motion and thus the shape of a particle need to be taken into account for accurate simulation of its motion [6].

Comprehensive particle size analysis may be standardized as specified in DIN ISO 9276-6. In this norm, properties of particle size distributions are precisely defined along with other parameters used for particle characterization [7]. Shape parameters are defined for two- and three dimensional descriptions of the particles. Parameters used in this work are equivalent diameters based on area and circumference of the particles as well as the minimum and maximum Feret diameters.

1.4 Experimental parameters

Table 1: Range of parameter variation for the experiments referred to in this report

Parameter	Variation range
Atmosphere	Air
Interacting surfaces	Pebble-Pebble-Pebble (p-p-p), Pebble-Wall (p-w)
Contact load	10 – 640 N
Rotational velocity	10 – 50 min^{-1}
Graphite grades	A 3, and SGL blind pebbles (type MLRF) / SGL NBG-17 graphite disc

Figure 4 is a photograph of the test facility showing the pebble mill and the electric motor on the right and the frequency inverter on the left. The grinding parts (here: ppp-contact) are enclosed in an acrylic containment in which the composition of the surrounding gas can be controlled.

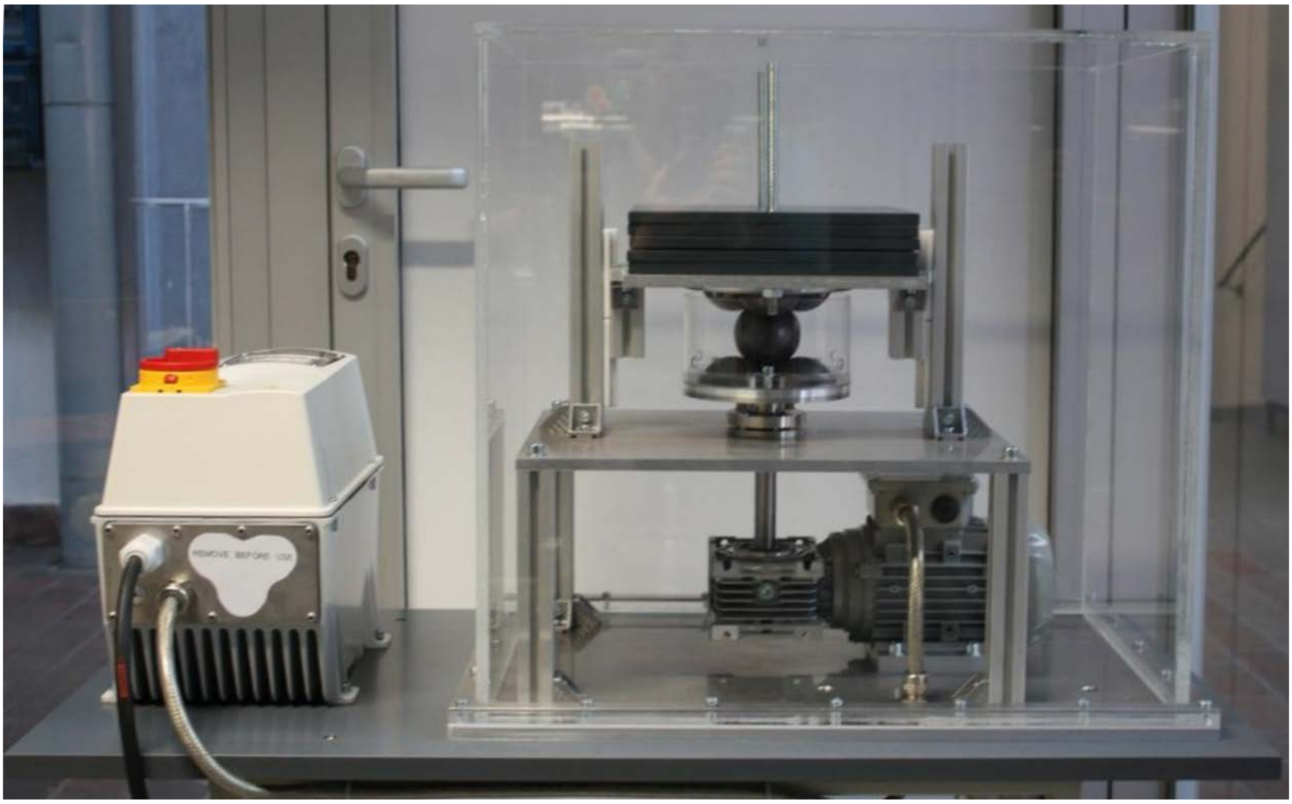

Figure 4: Test facility pebble mill (left: frequency converter)

Table 2: Load scenarios investigated in this work

Load scenario	graphite grade *A3*	graphite grade *MLRF*
80 N (constant)	x	x
160N (constant)	x	x
320N (constant)	x	x
640 N (constant))	x	x
80-640 N (continuously increasing)	x	x
160 N (grinding on NBG-17 disc)	x	-

After each experiment, the pebbles were discharged from the pebble mill and the generated graphite particles were carefully removed both from the apparatus and the pebbles using an ethanol solution. For each sample, the following parameters were determined:

- particle size distribution and cumulative size distribution,
- median particle diameter based on the cumulative particle area,
- aspect ratio as defined in DIN ISO 9276-6 and, alternatively, using the Ferret diameters,
- circularity.

The results of these analyses, as listed in Table 2, are documented in the chapters 2, 3, 4, and 5, followed by a discussion in chapter 6.

2 Results of friction experiments using MLRF pebbles

After completion of each experiment, the generated graphite particles were collected from the test chamber and thoroughly analysed with respect to their size and shape. Based on these data, particle size distributions and shape distributions have been derived, which are given below. In case of the first load scenario 2.1 (160 N, 27.5 Hz rotational frequency, MLRF pebbles), the first figure (Figure 5) shows the discrete particle size distribution, and the second figure (Figure 6) shows both the number-weighted and area-weighted cumulative size distributions. The third figure (Figure 7) is a scatter plot of particle aspect ratio versus particle size for all particles under investigation, which is summarized in the distribution shown in Figure 8. In Figure 9, the circularity of particles is shown versus the particle size in another scatter plot. These evaluations have been performed for all experiments, respectively, and are documented in this deliverable consistently in the same manner. In this regard, 5 Figures are given for each experimental run documented in chapter 2, 3, and chapter 5.

2.1 Load of 160 N at 27.5 Hz rotational frequency (MLRF pebble)

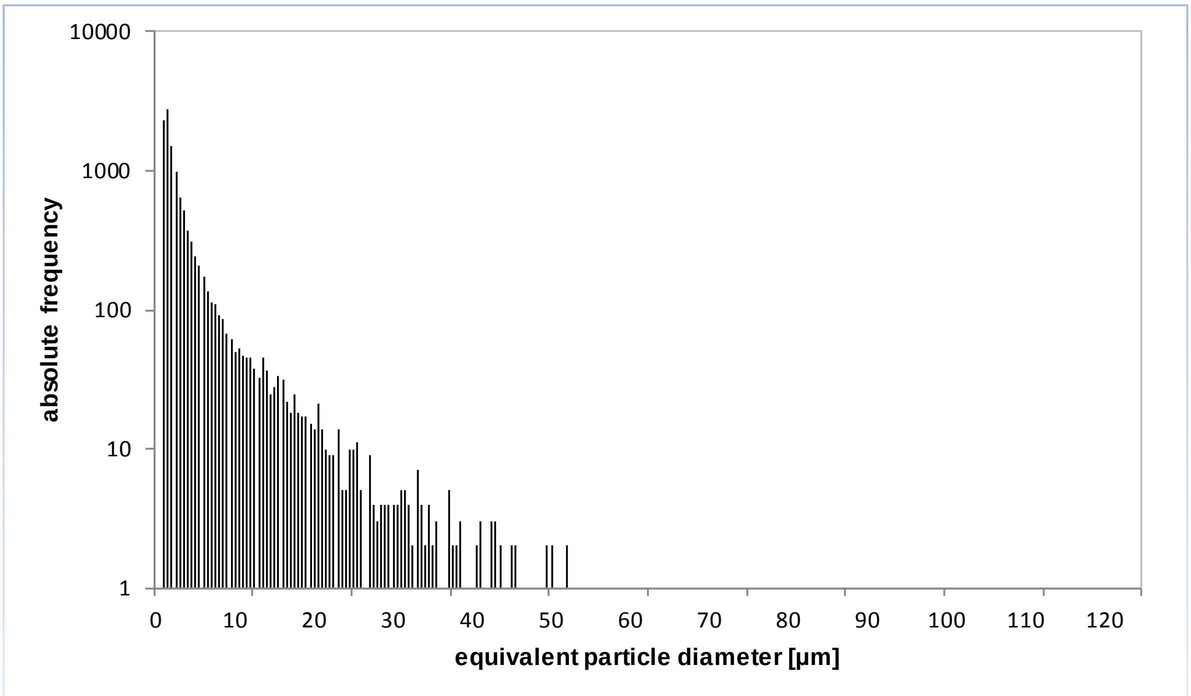

Figure 5: Particle size distribution of particles generated at 160 N /27.5 Hz (MLRF pebble)

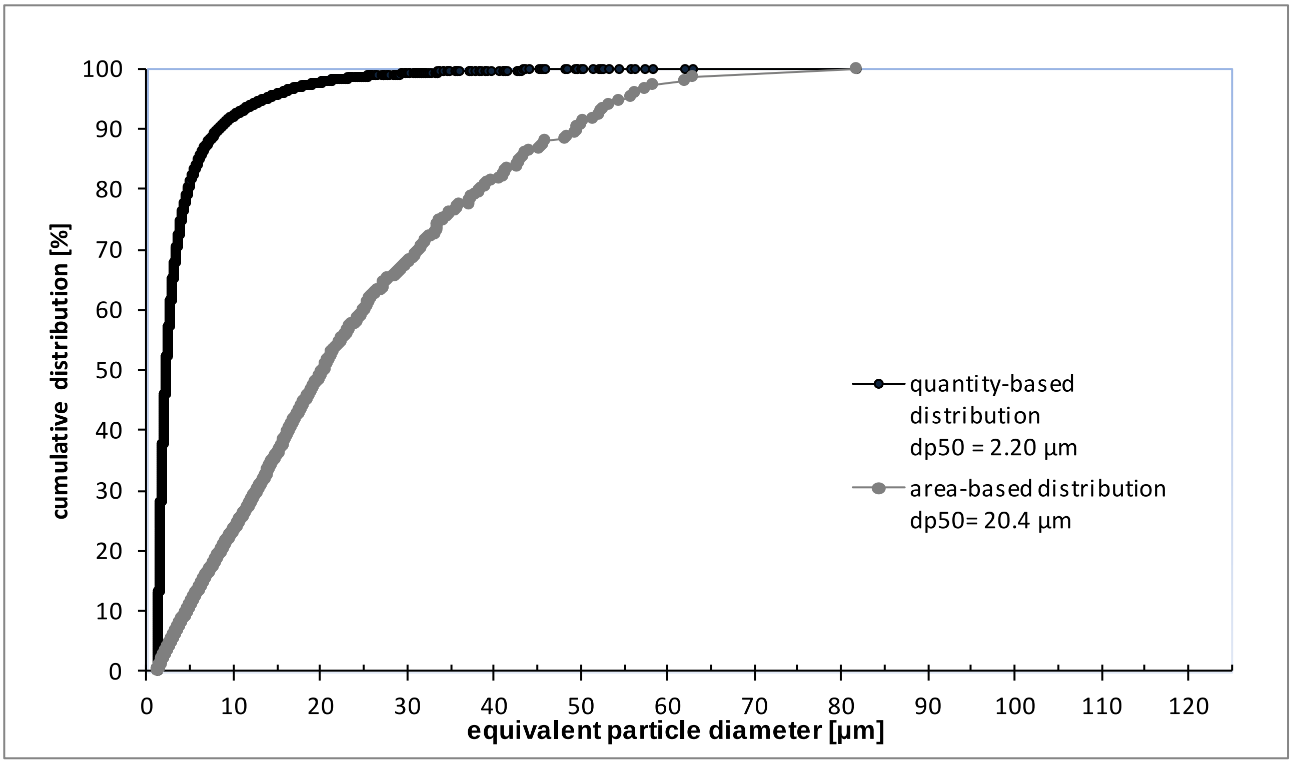

Figure 6: Cumulative particle size distribution of particles generated at 160 N/27.5 Hz (MLRF pebble)

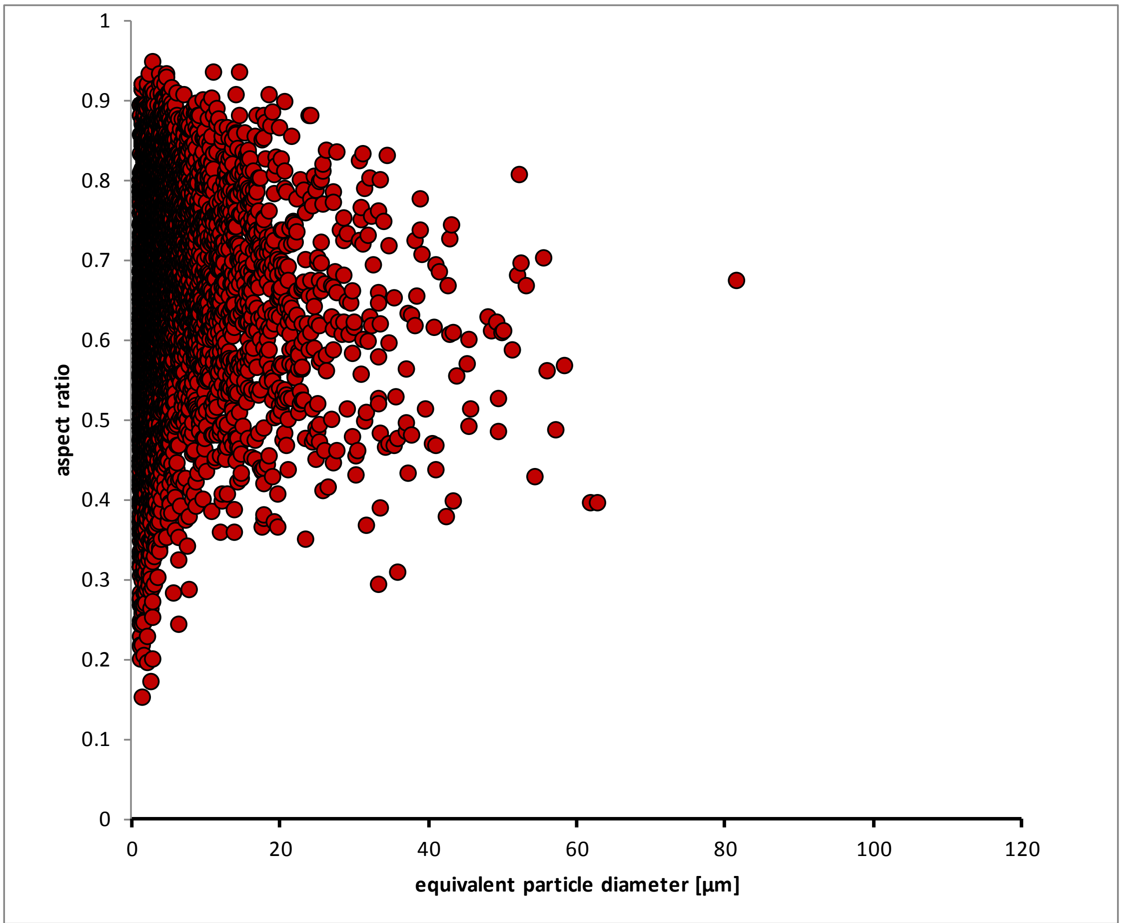

Figure 7: Aspect ratio of particles generated at 160 N/27.5 HZ (MLRF pebble)

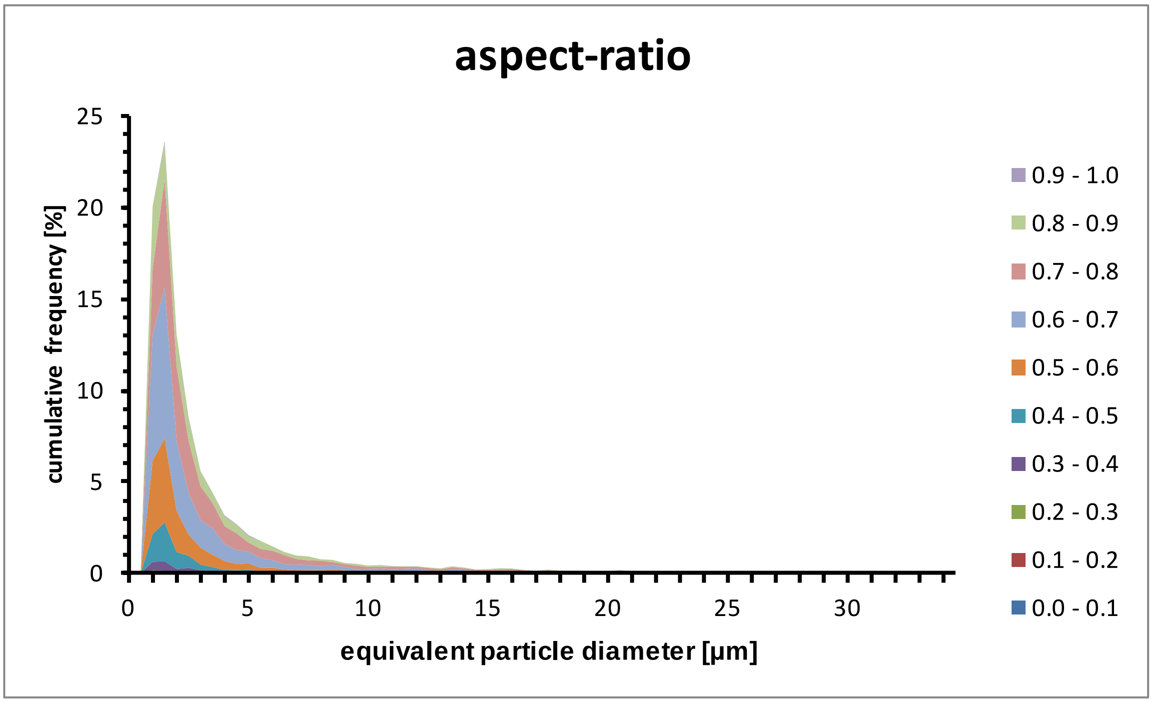

Figure 8: Distribution of the aspect ratio of particles generated at 160 N/27.5 Hz (MLRF pebble)

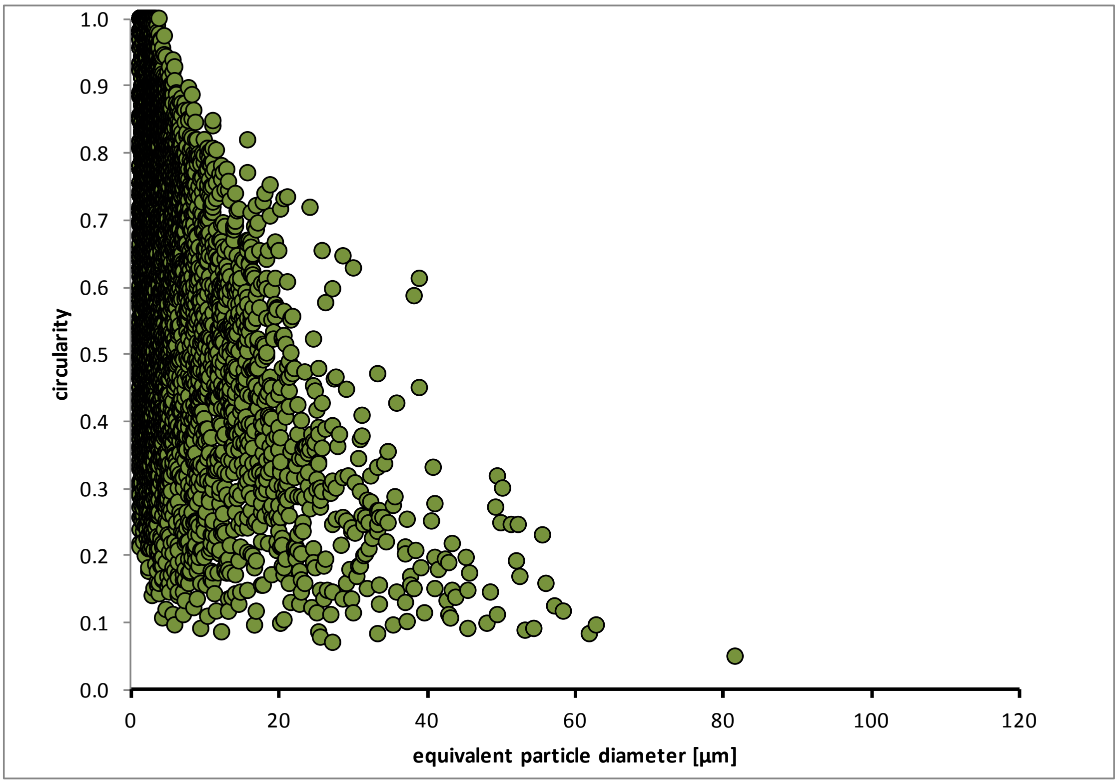

Figure 9: Overview of size and circularity of the particles under investigation (160 N/27.5 Hz, MLRF pebble)

2.2 Load of 160 N at 5.5 Hz rotational frequency (MLRF pebble)

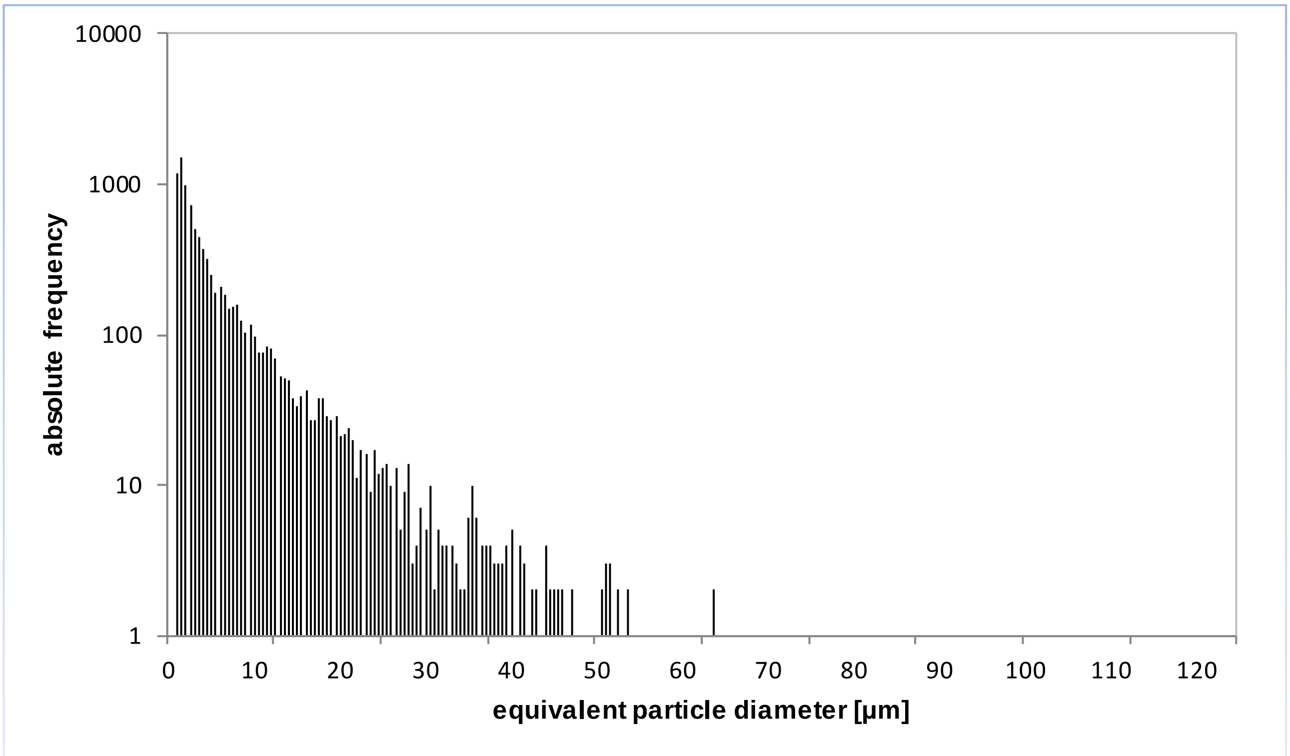

Figure 10: Particle size distribution of particles generated at 160 N /5.5 Hz (MLRF pebble)

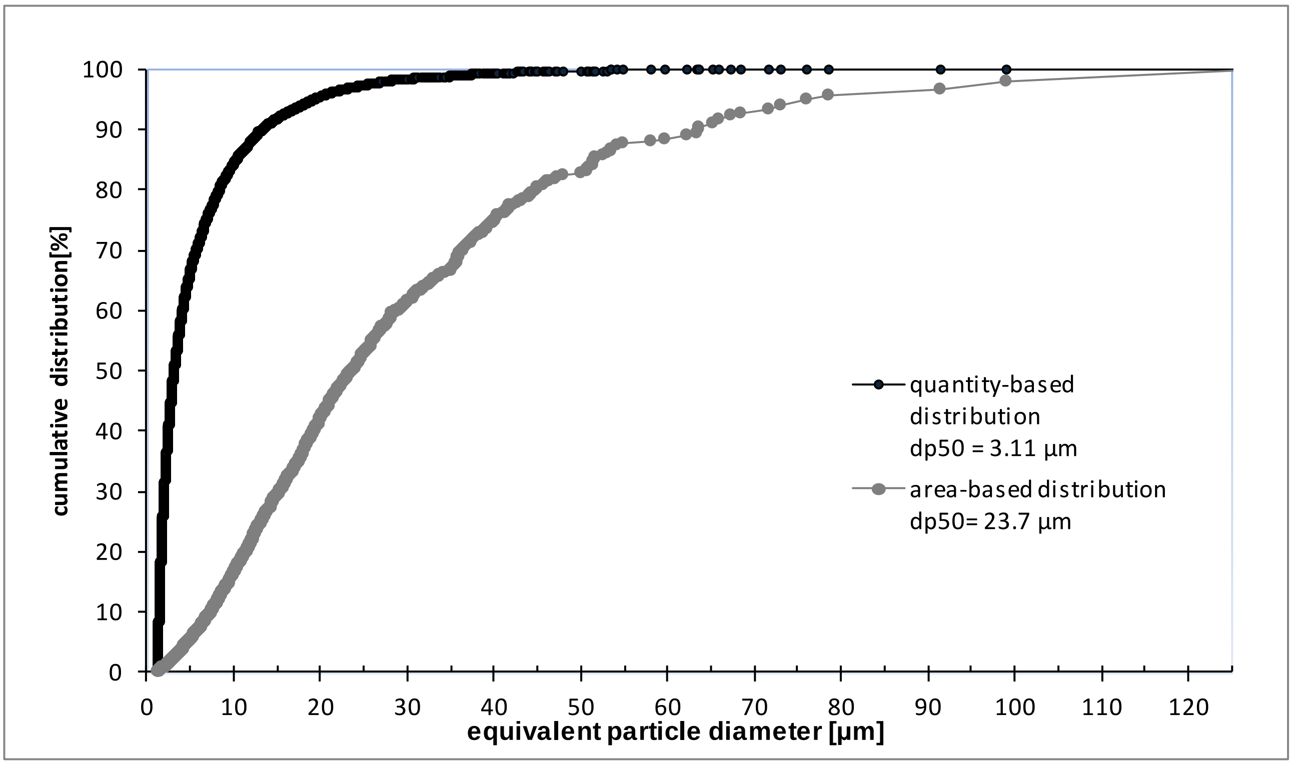

Figure 11: Cumulative particle size distribution of particles generated at 160 N/5.5 Hz (MLRF pebble)

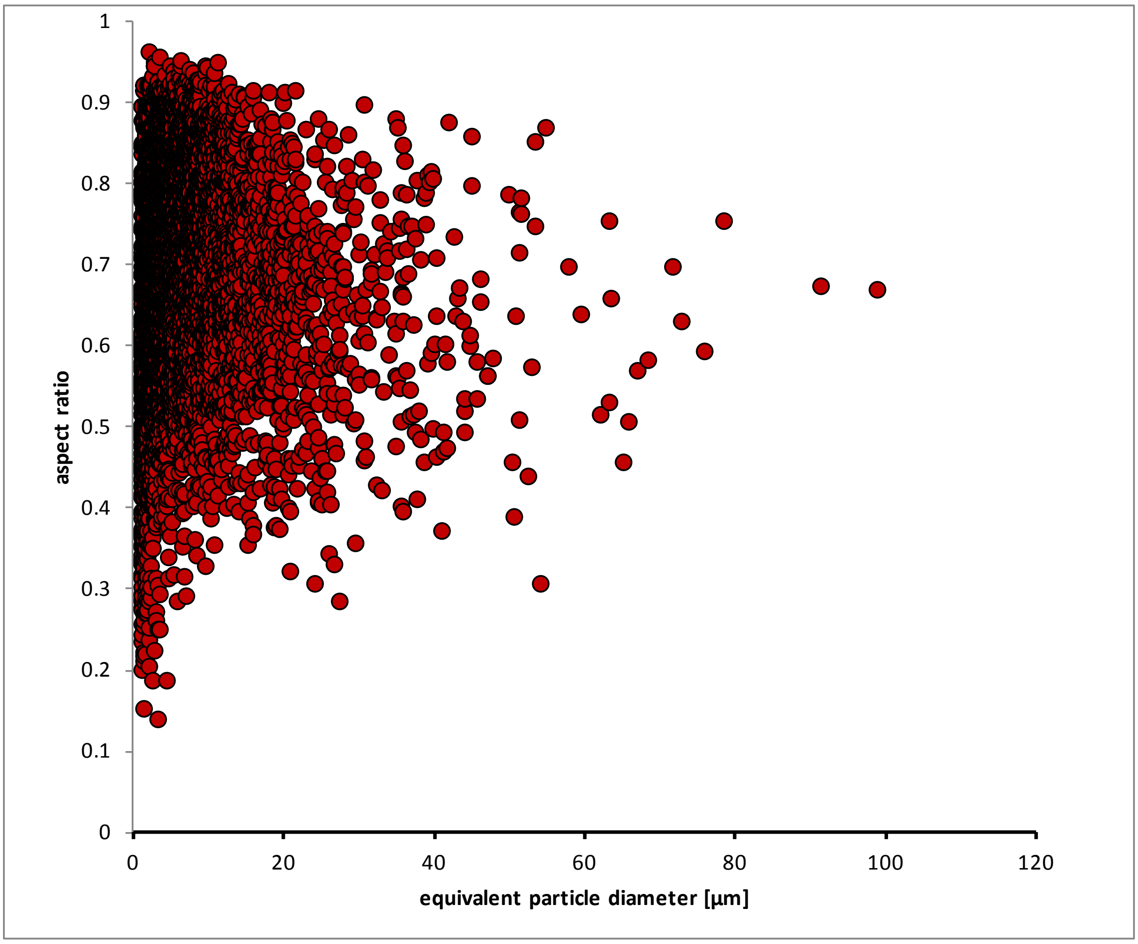

Figure 12: Aspect ratio of particles generated at 160 N/5.5 HZ (MLRF pebble)

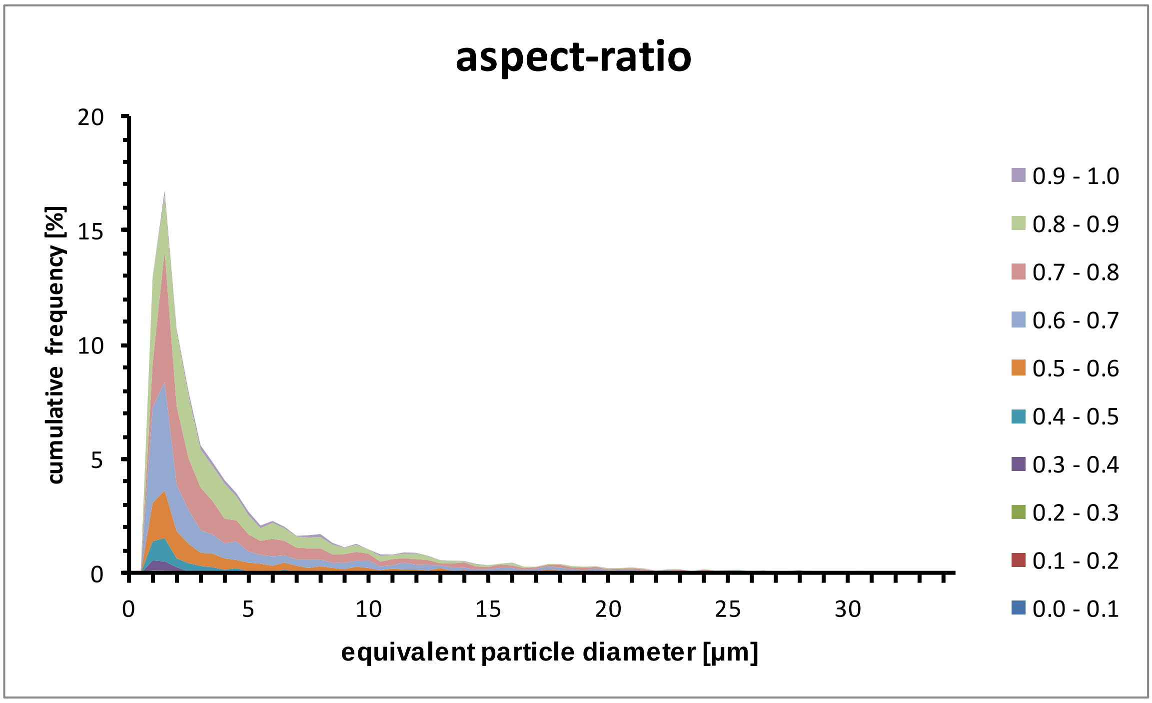

Figure 13: Distribution of the aspect ratio of particles generated at 160 N/5.5 Hz (MLRF pebble)

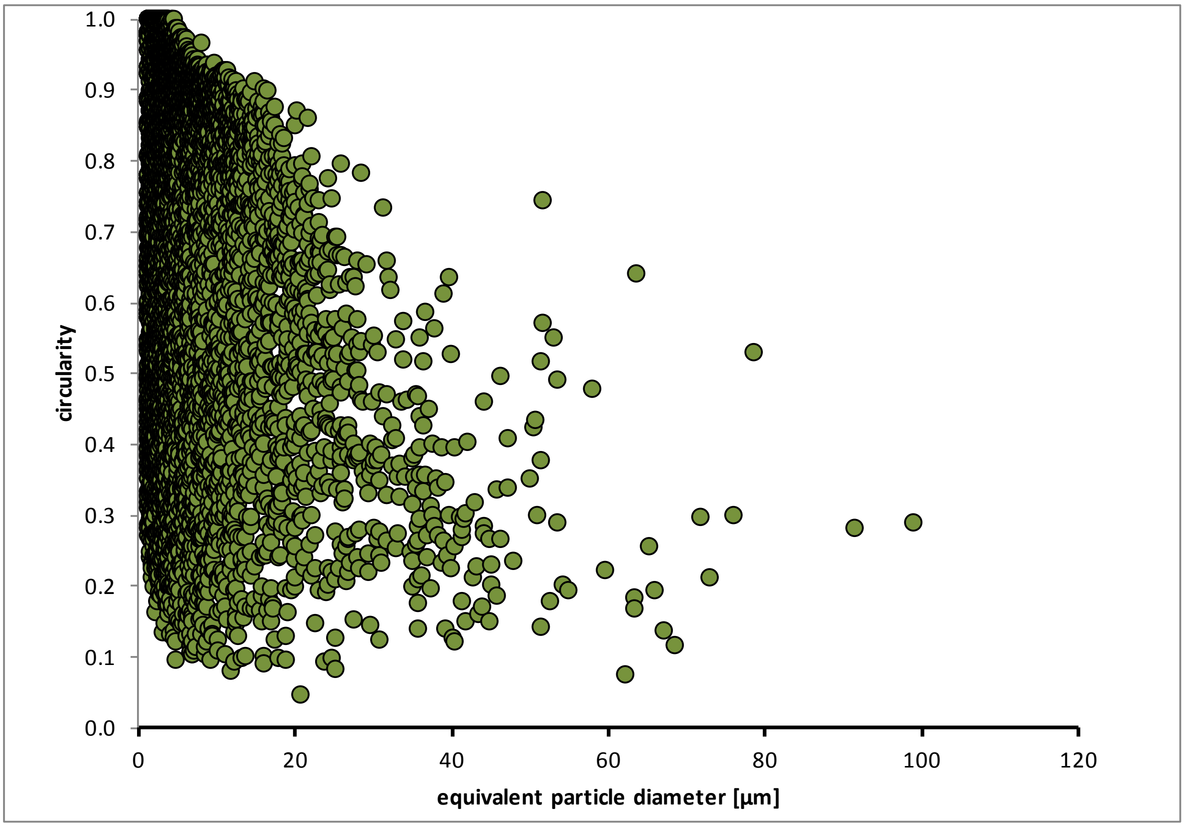

Figure 14: Overview of size and circularity of the particles under investigation (160 N/5.5 Hz, MLRF pebble)

2.3 Load of 320 N at 27.5 Hz rotational frequency (MLRF pebble)

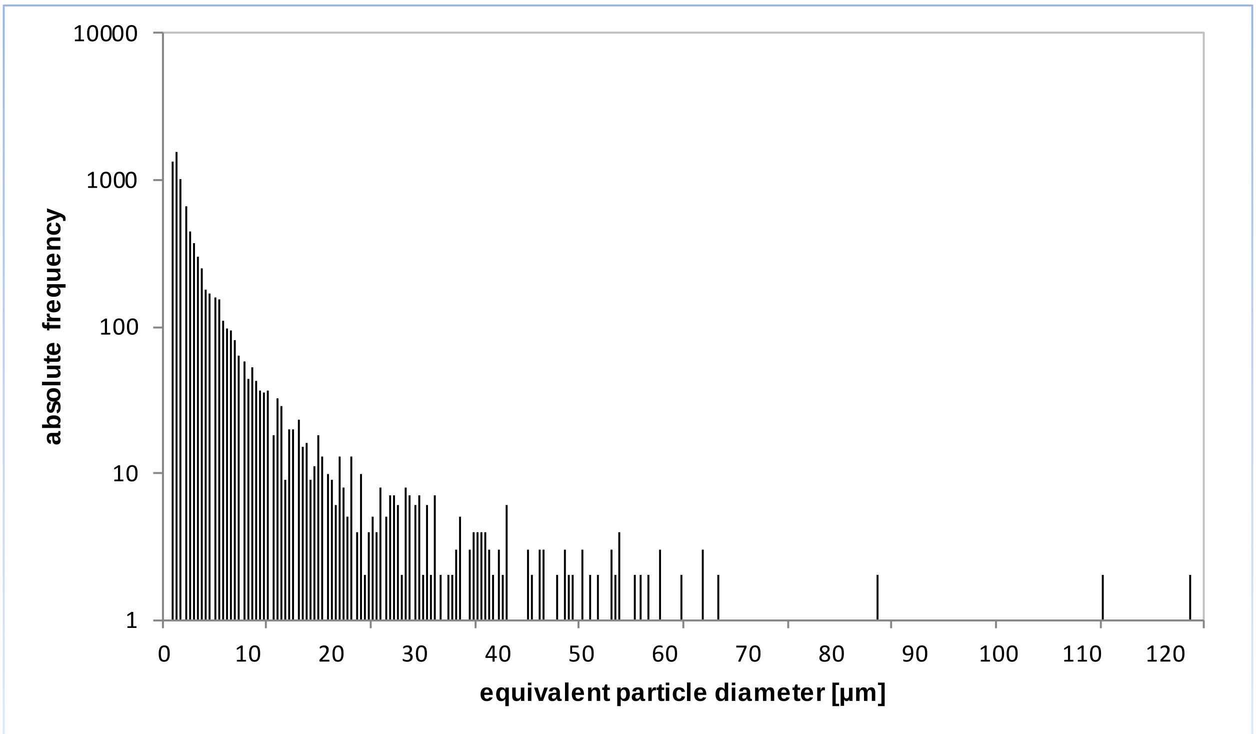

Figure 15: Particle size distribution of particles generated at 320 N /27.5 Hz (MLRF pebble)

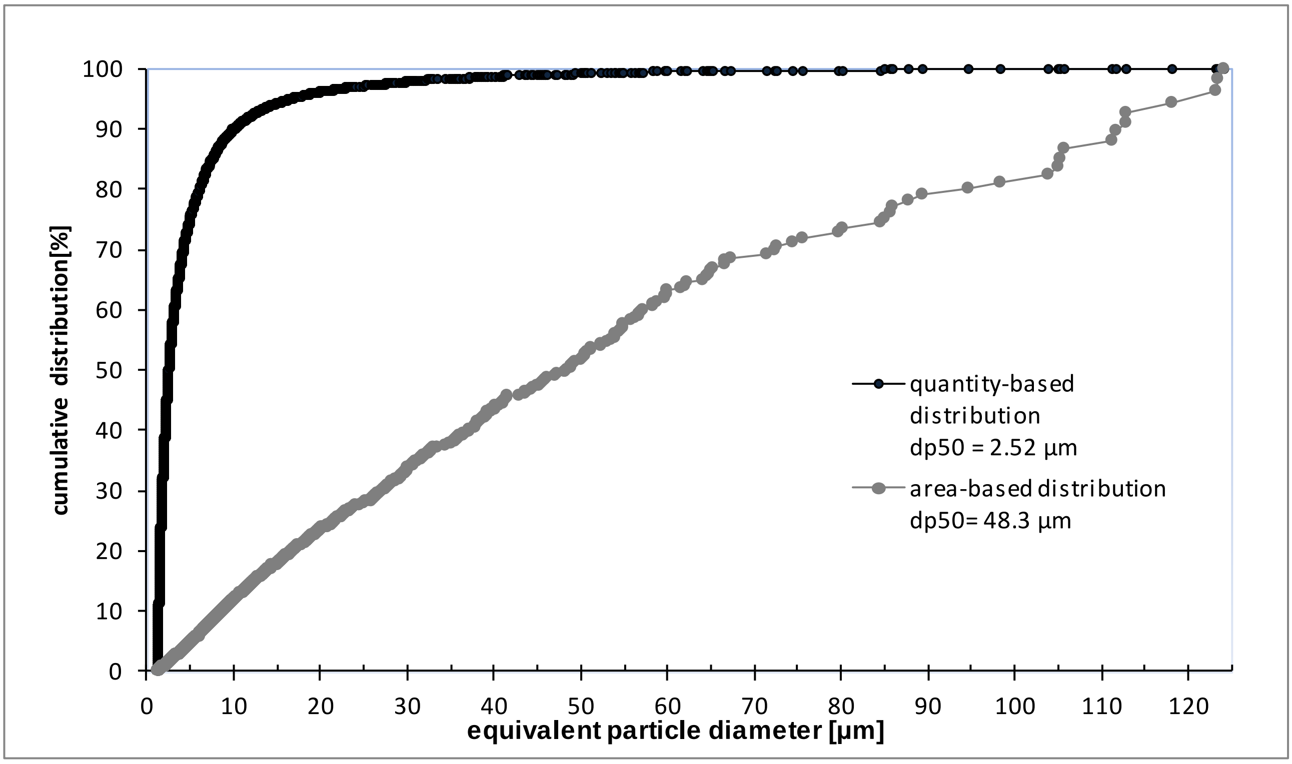

Figure 16: Cumulative particle size distribution of particles generated at 320 N/27.5 Hz (MLRF pebble)

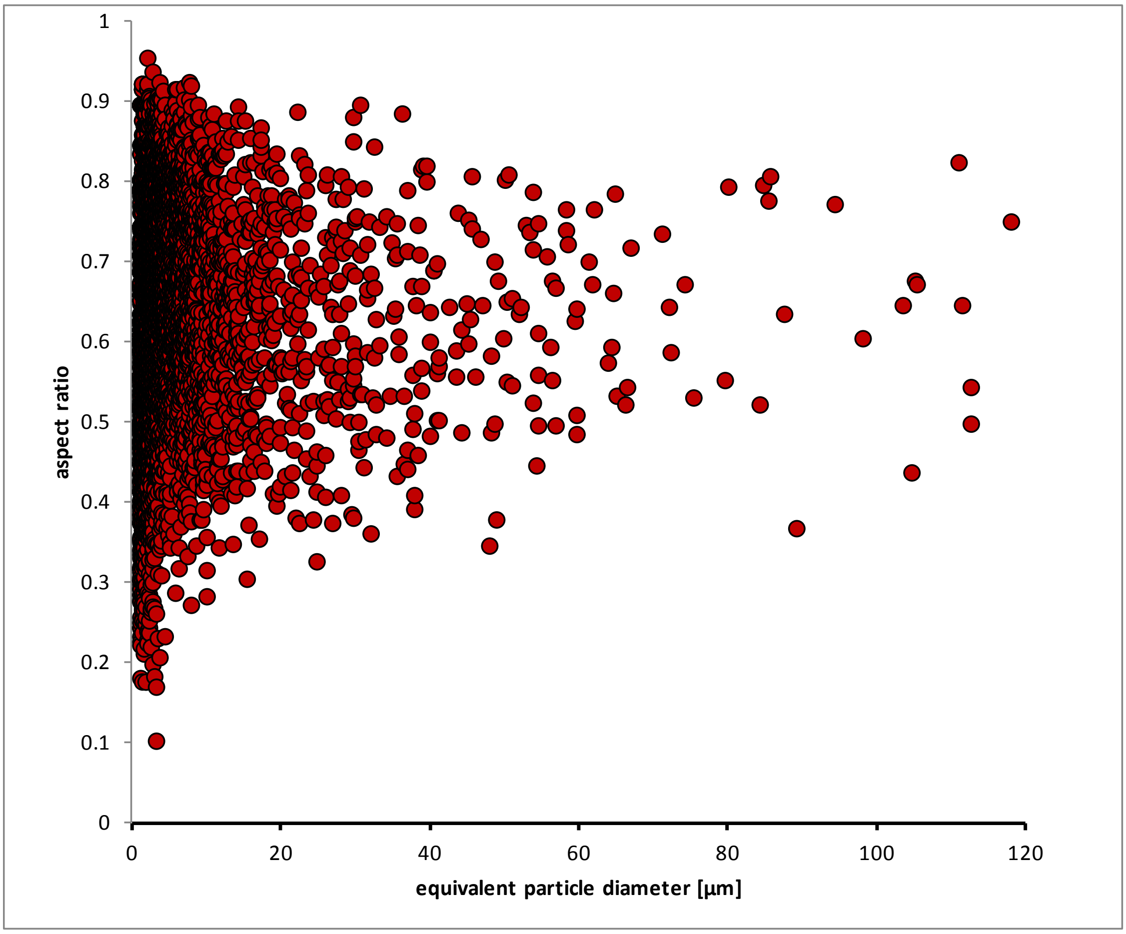

Figure 17: Aspect ratio of particles generated at 320 N/27.5 HZ (MLRF pebble)

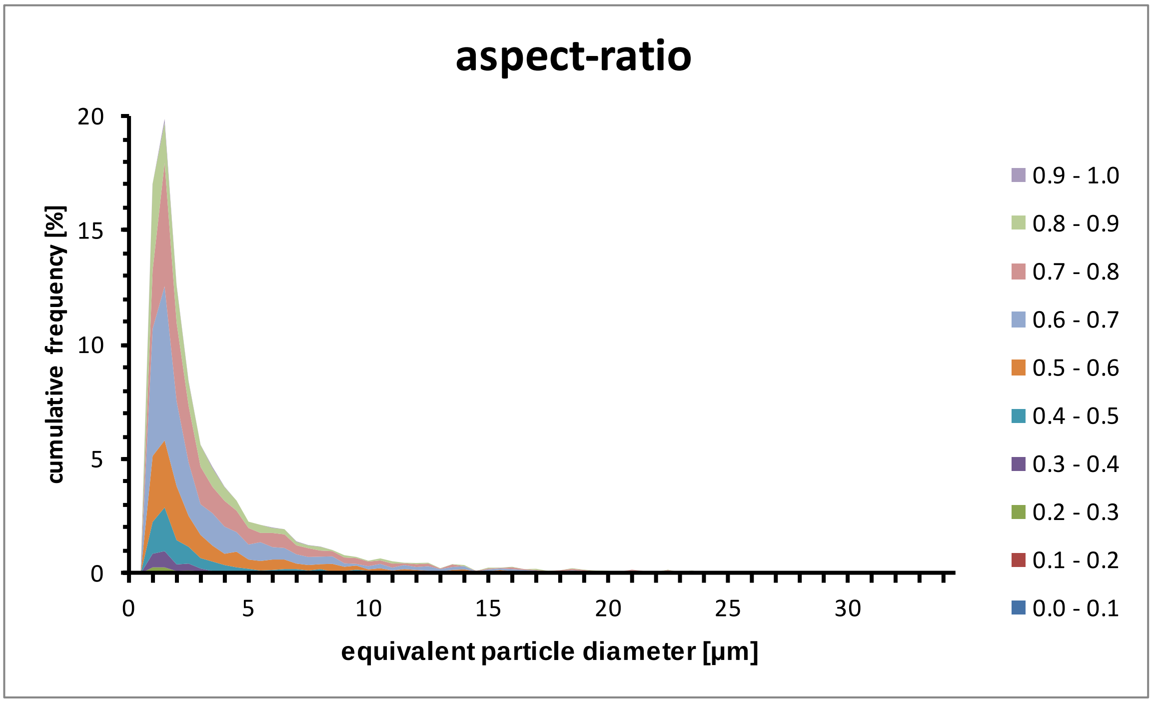

Figure 18: Distribution of the aspect ratio of particles generated at 320 N/27.5 Hz (MLRF pebble)

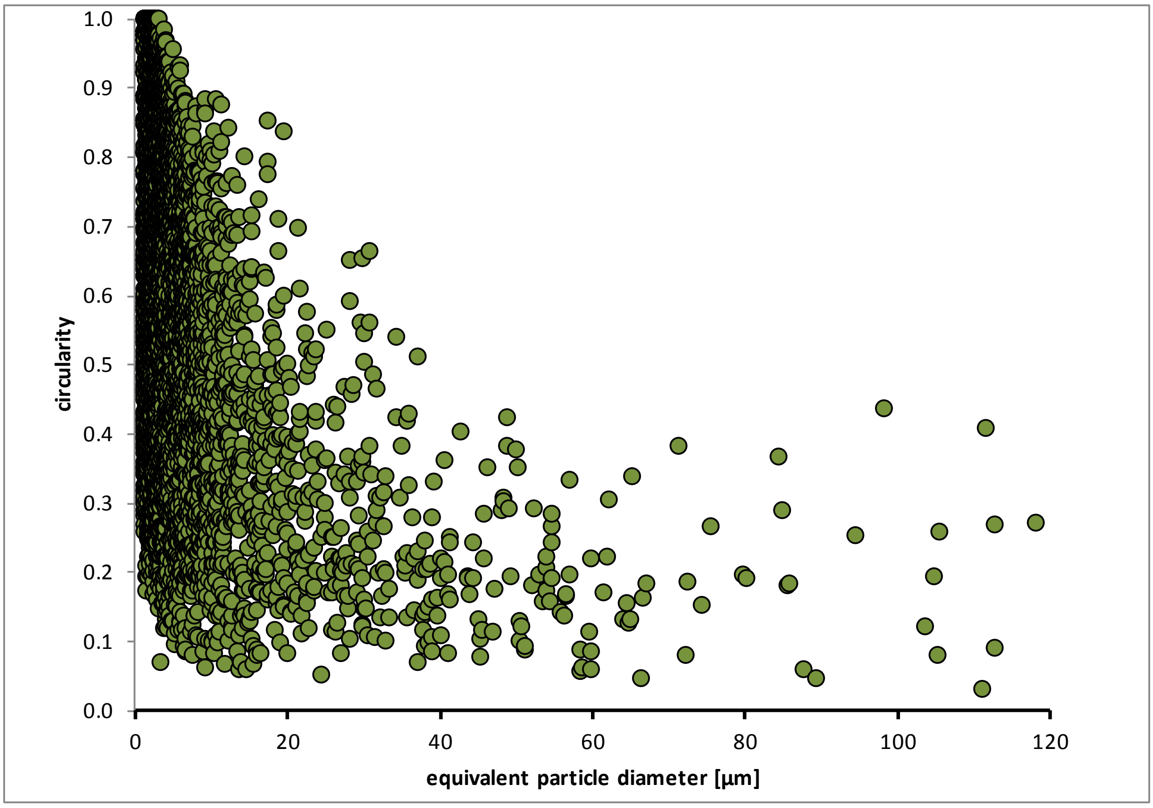

Figure 19: Overview of size and circularity of the particles under investigation (320 N/27.5 Hz, MLRF pebble)

2.4 Load of 640 N at 27.5 Hz rotational frequency (MLRF pebble)

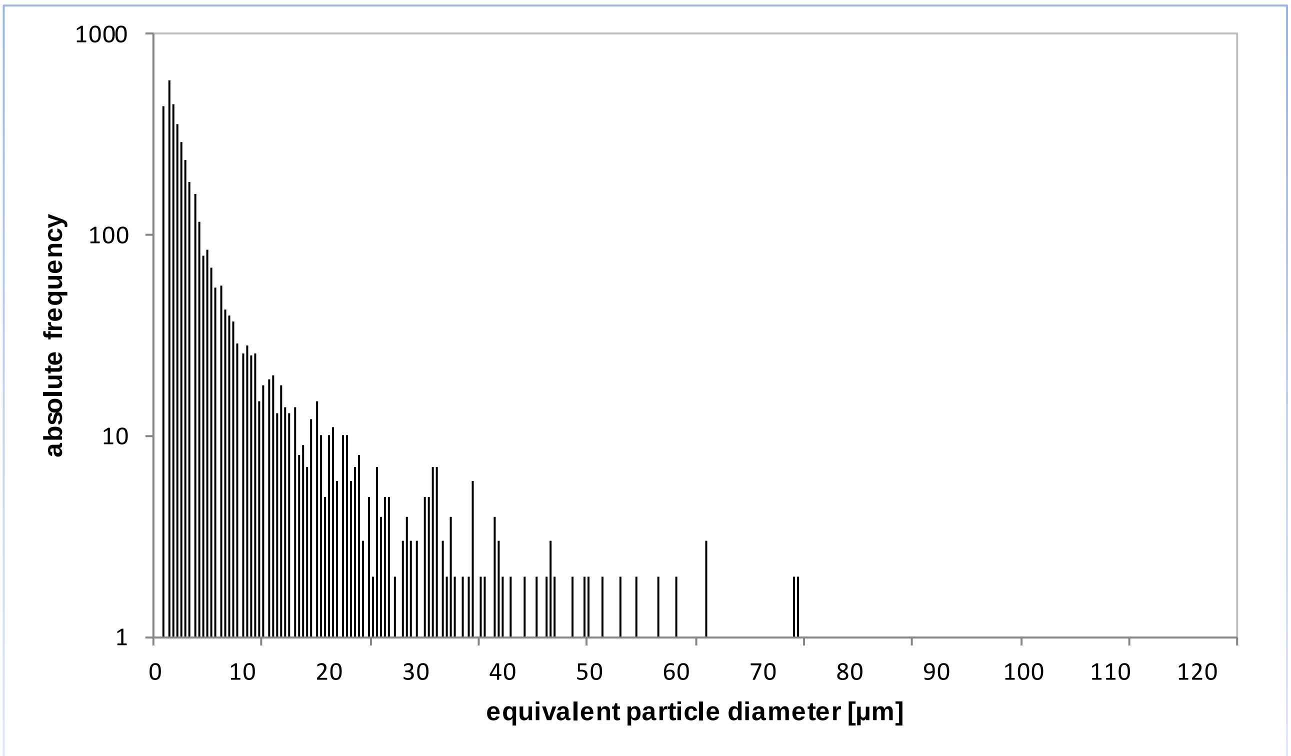

Figure 20: Particle size distribution of particles generated at 640 N /27.5 Hz (MLRF pebble)

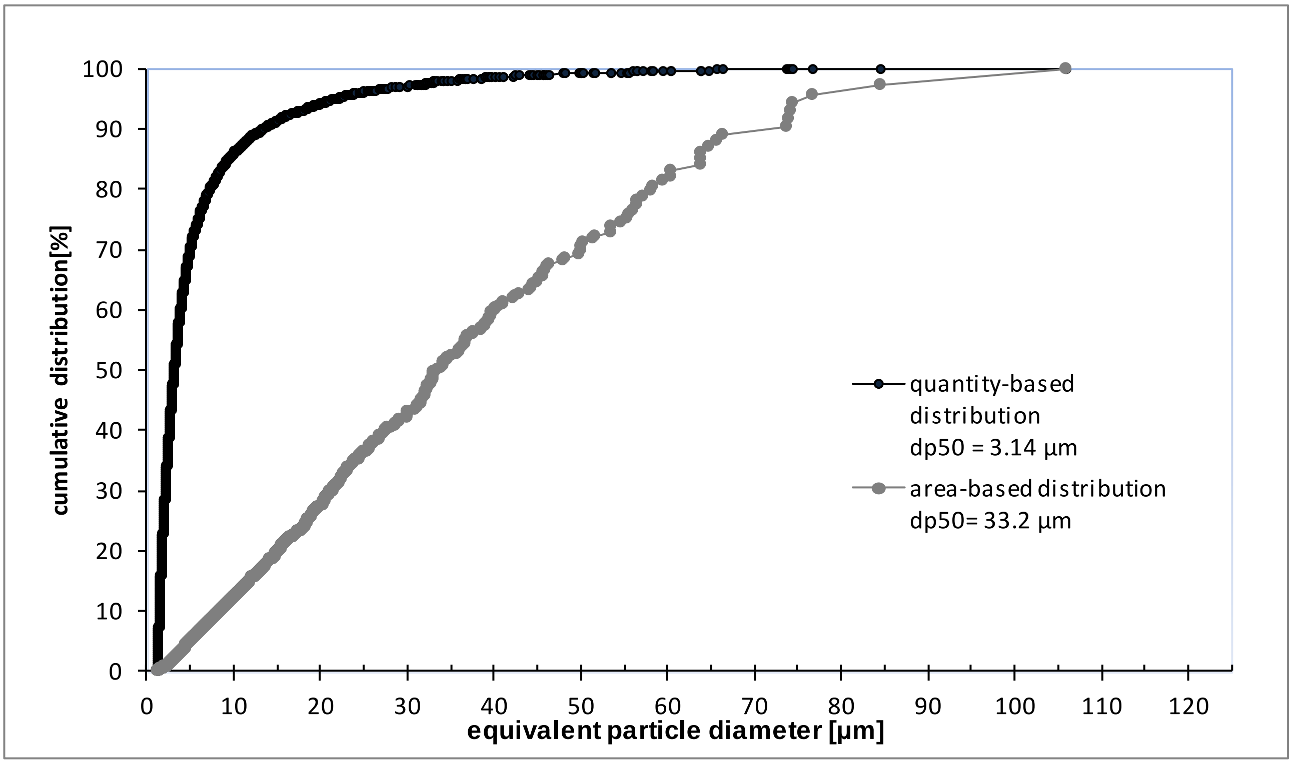

Figure 21: Cumulative particle size distribution of particles generated at 640 N/27.5 Hz (MLRF pebble)

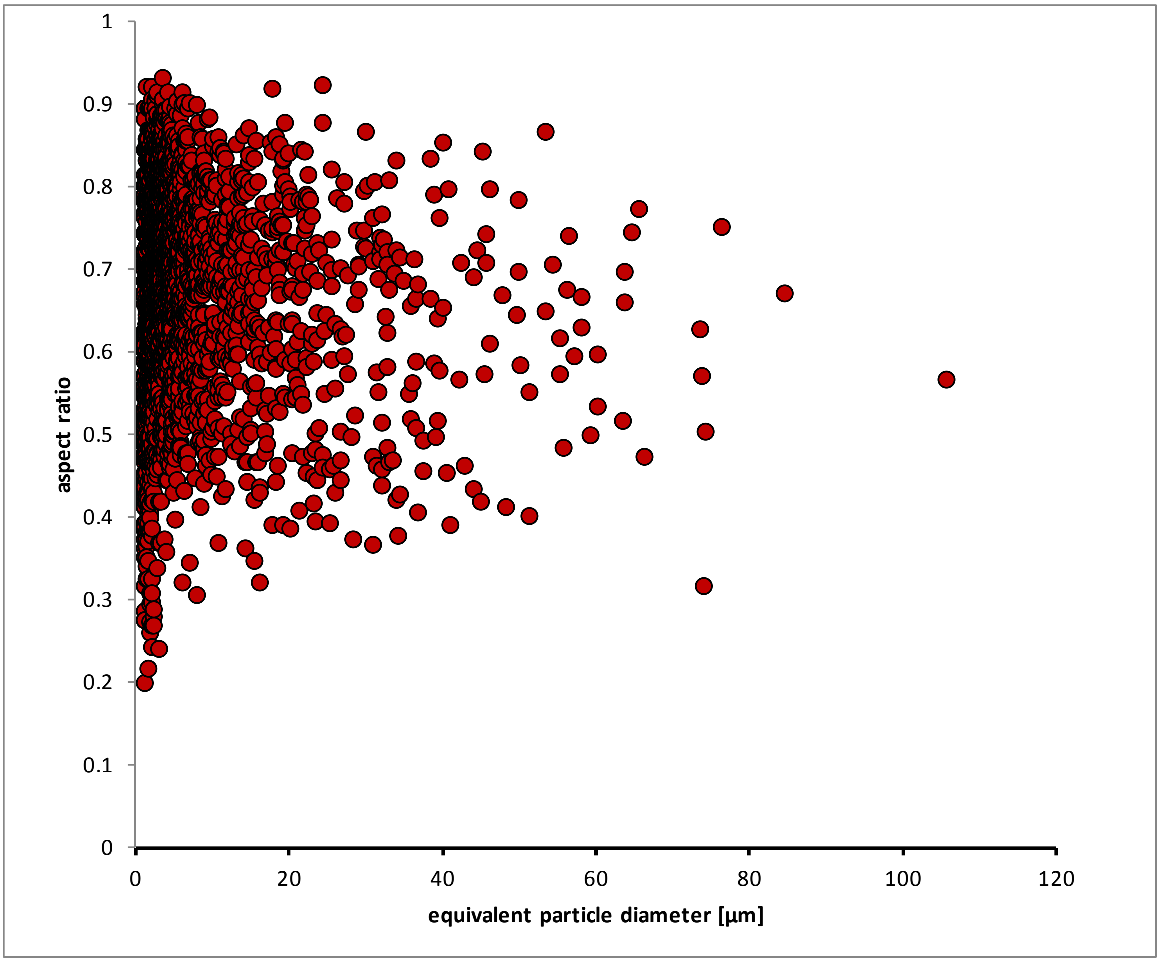

Figure 22: Aspect ratio of particles generated at 640 N/27.5 HZ (MLRF pebble)

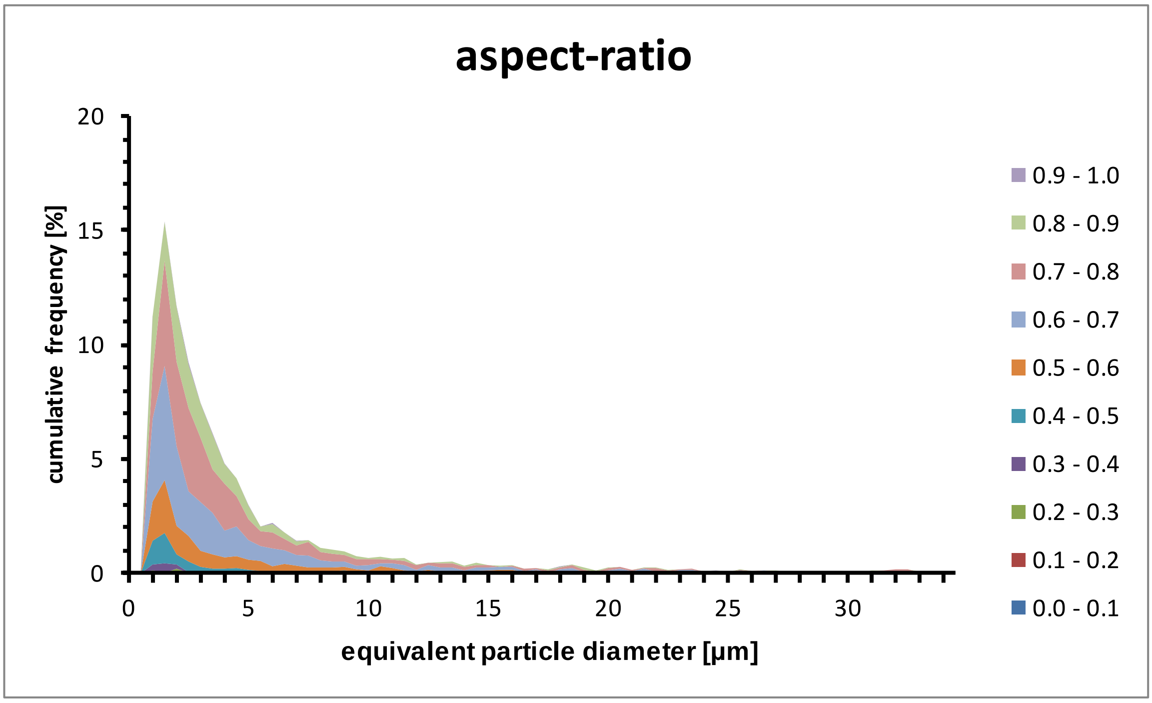

Figure 23: Distribution of the aspect ratio of particles generated at 640 N/27.5 Hz (MLRF pebble)

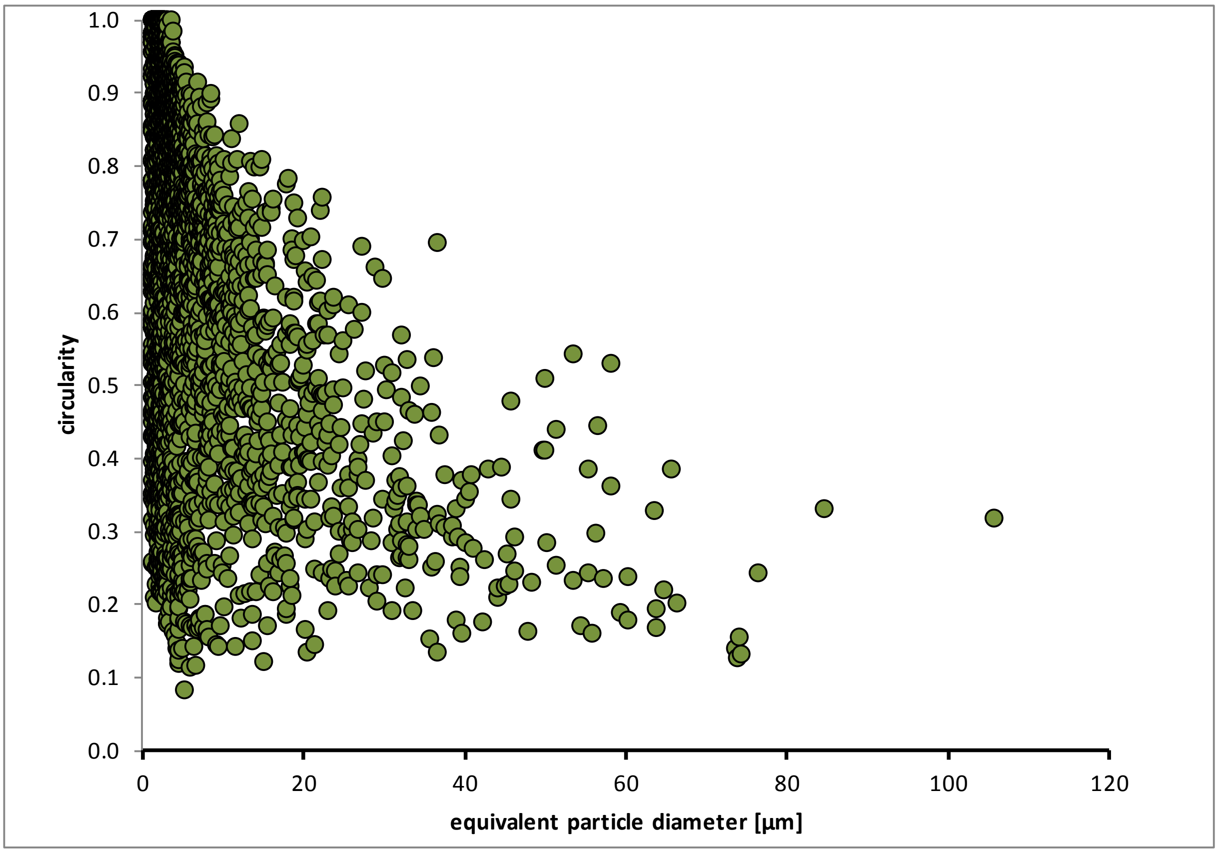

Figure 24: Overview of size and circularity of the particles under investigation (640 N/27.5 Hz, MLRF pebble)

3 Results of friction experiments using A3 pebbles

The evaluation of particles generated by abrasion of A3 graphite pebbles were performed in the same manner as described for particles generated by abrasion of MLRF pebbles described in chapter 2. For each experimental run, discrete and cumulative particle size distributions were determined (the first and second figure, respectively) as well as the particle aspect ratio (third and fourth figure, respectively), and the particle circularity (fifth figure).

3.1 Load of 80 N at 27.5 Hz rotational frequency (A3 pebble)

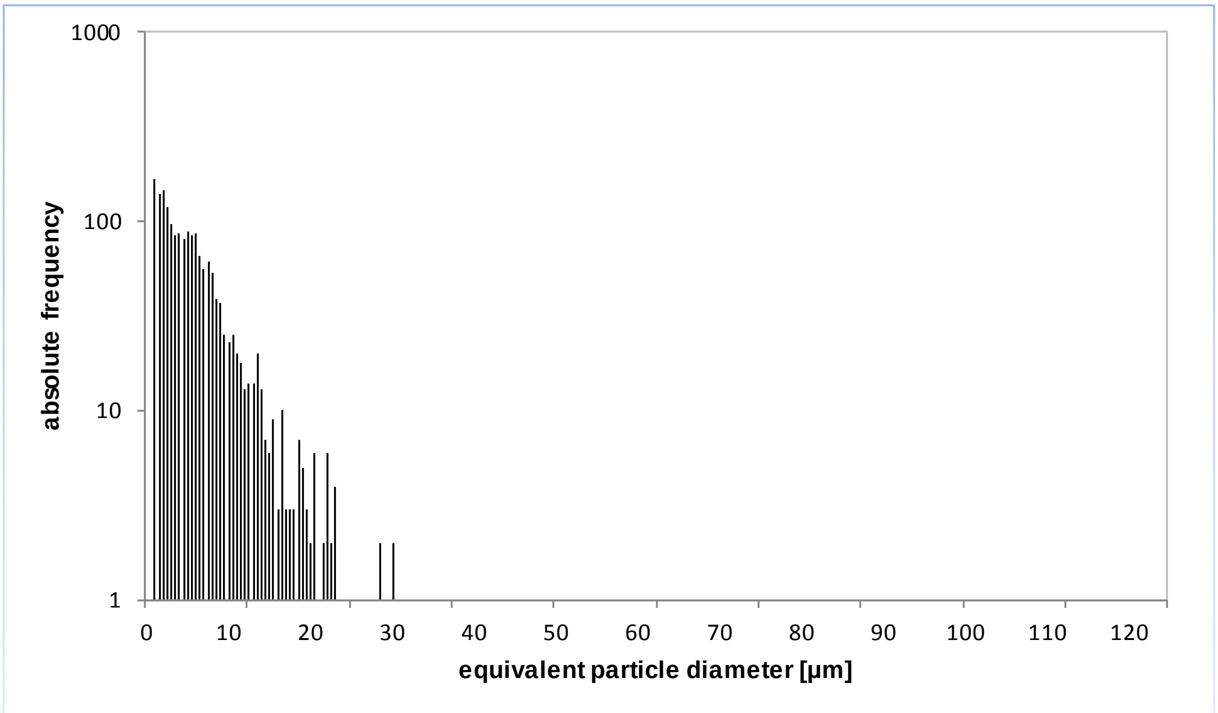

Figure 25: Particle size distribution of particles generated at 80 N /27.5 Hz (A3 pebble)

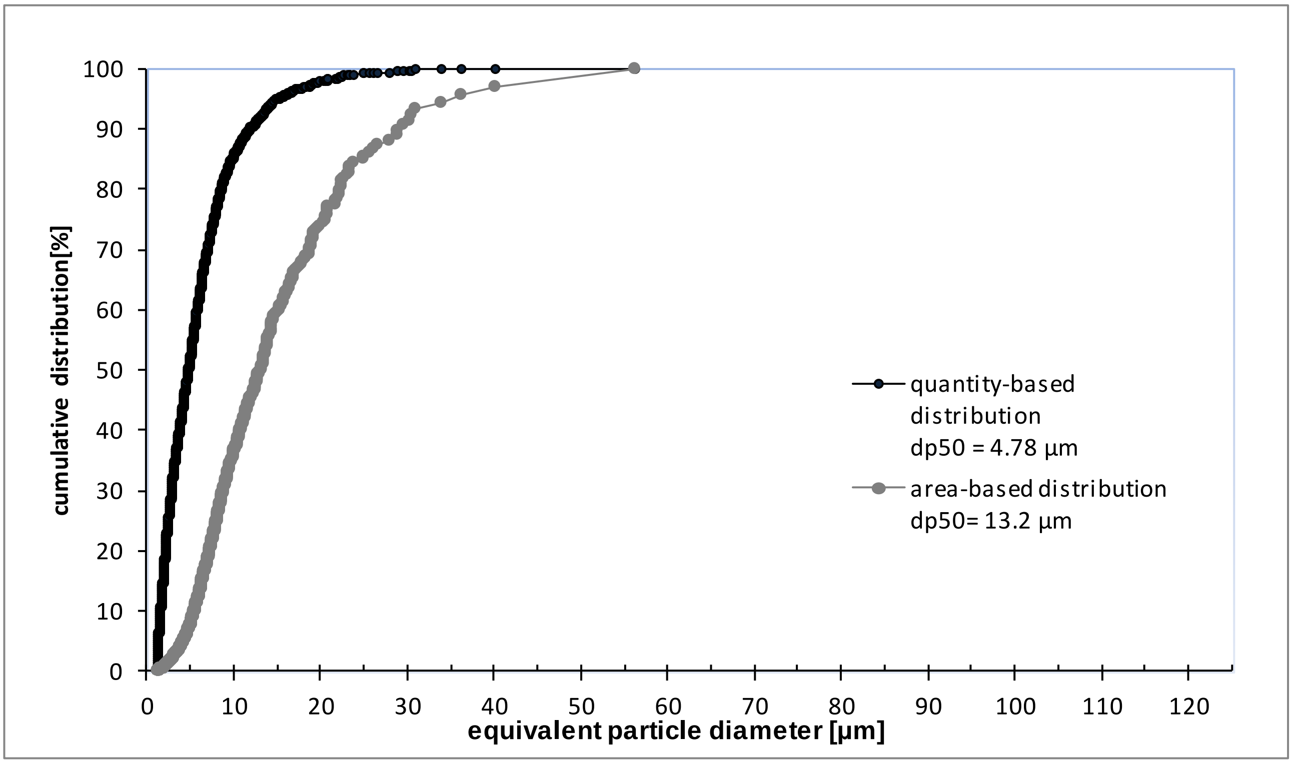

Figure 26: Cumulative particle size distribution of particles generated at 80 N/27.5 Hz (A3 pebble)

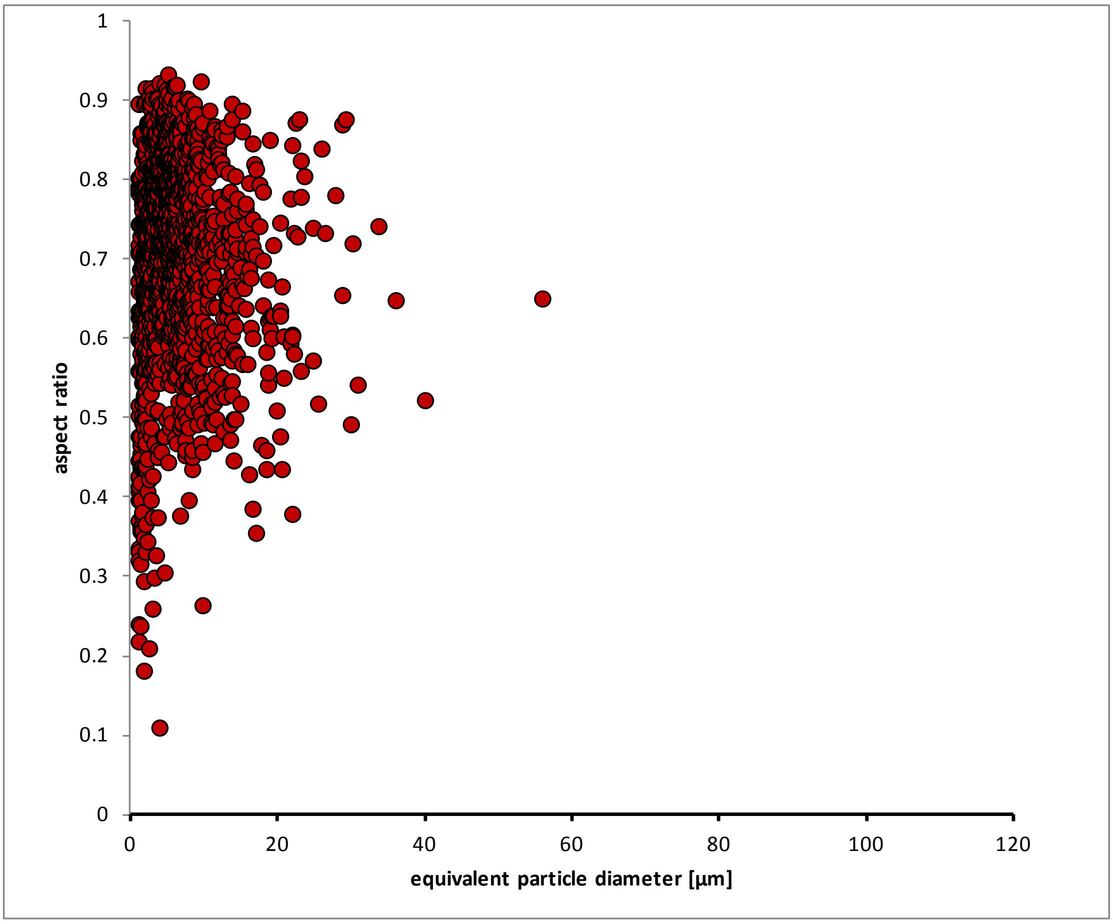

Figure 27: Aspect ratio of particles generated at 80 N/27.5 HZ (A3 pebble)

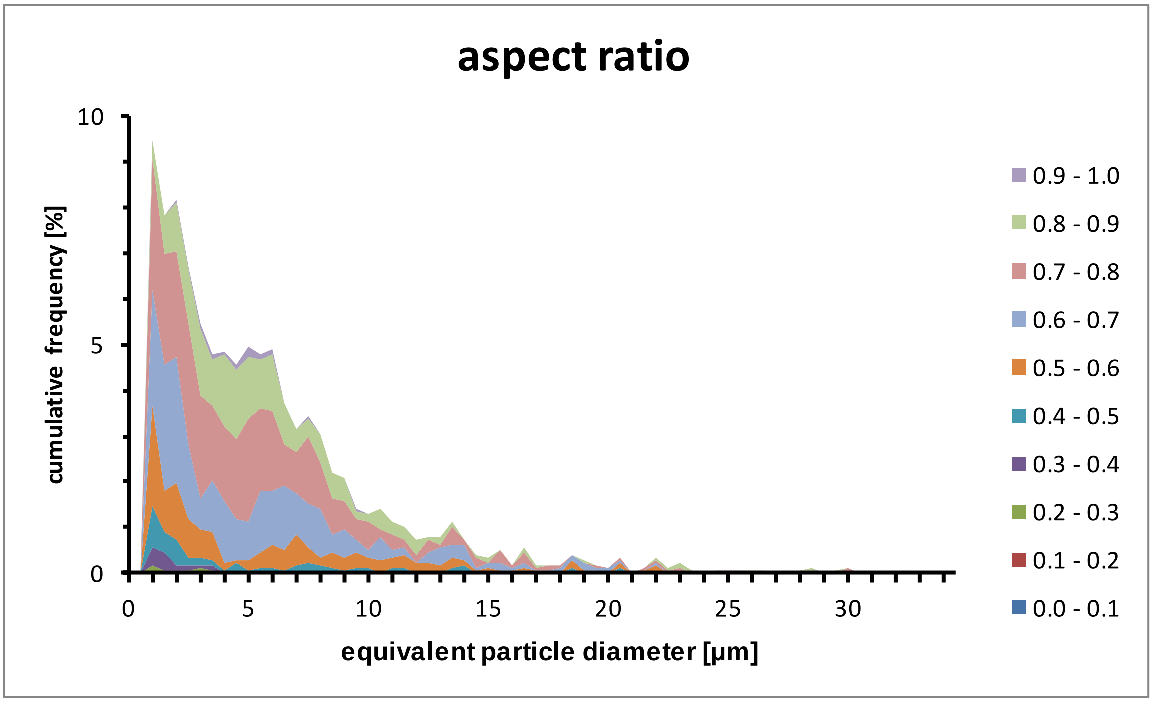

Figure 28: Distribution of the aspect ratio of particles generated at 80 N/27.5 Hz (A3 pebble)

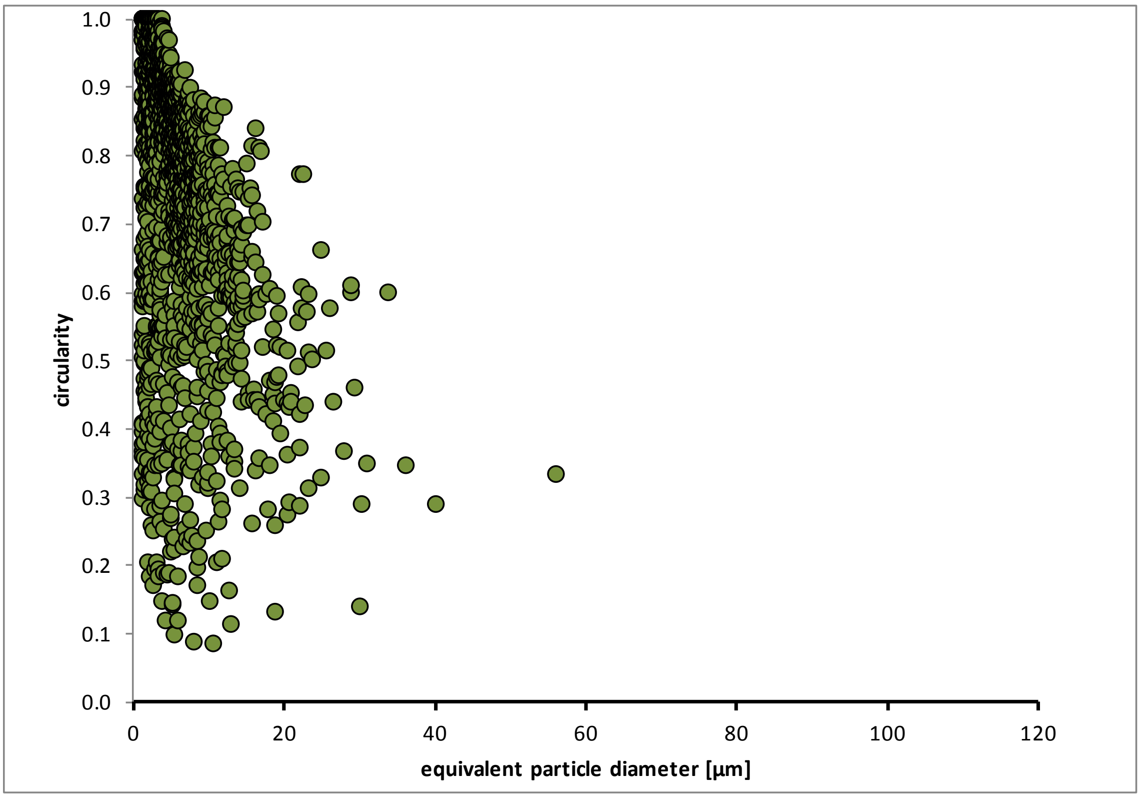

Figure 29: Overview of size and circularity of the particles under investigation (80 N/27.5 Hz, A3 pebble)

3.2 Load of 160 N at 27.5 Hz rotational frequency (A3 pebble)

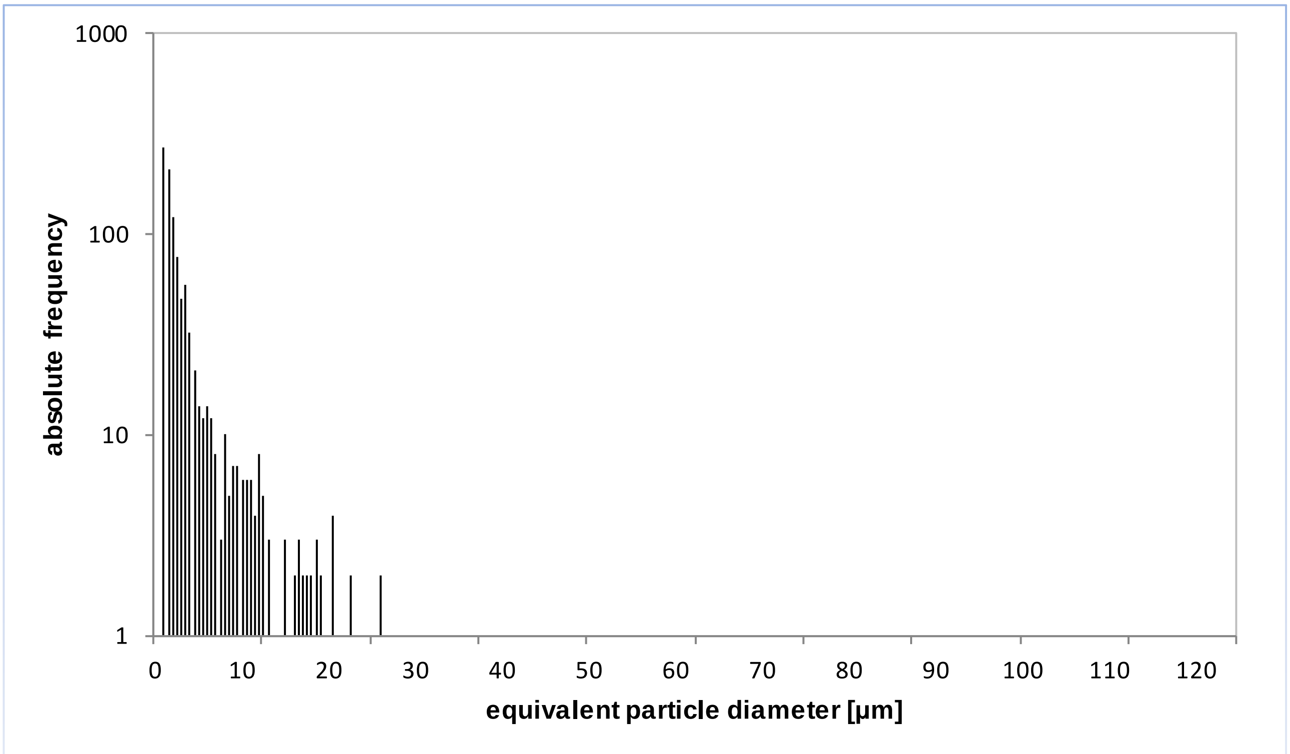

Figure 30: Particle size distribution of particles generated at 160 N /27.5 Hz (A3 pebble)

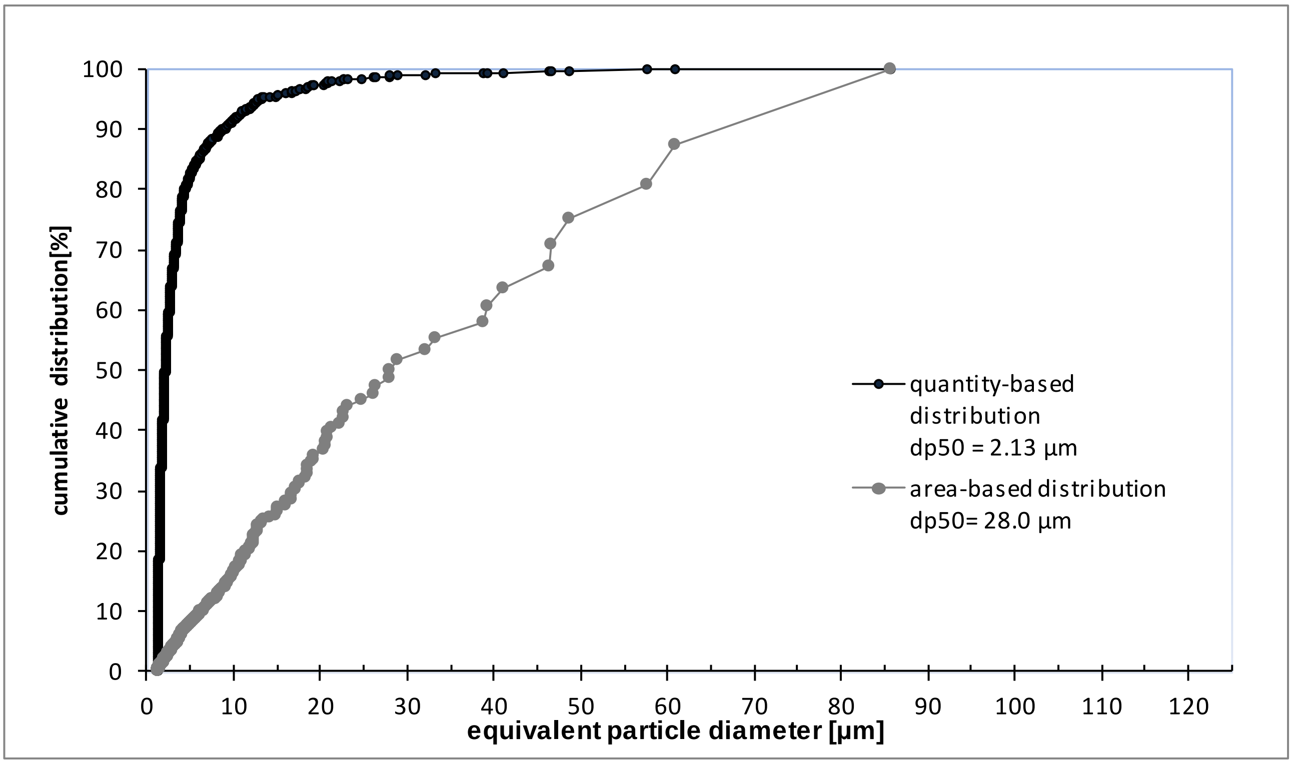

Figure 31: Cumulative particle size distribution of particles generated at 160 N/27.5 Hz (A3 pebble)

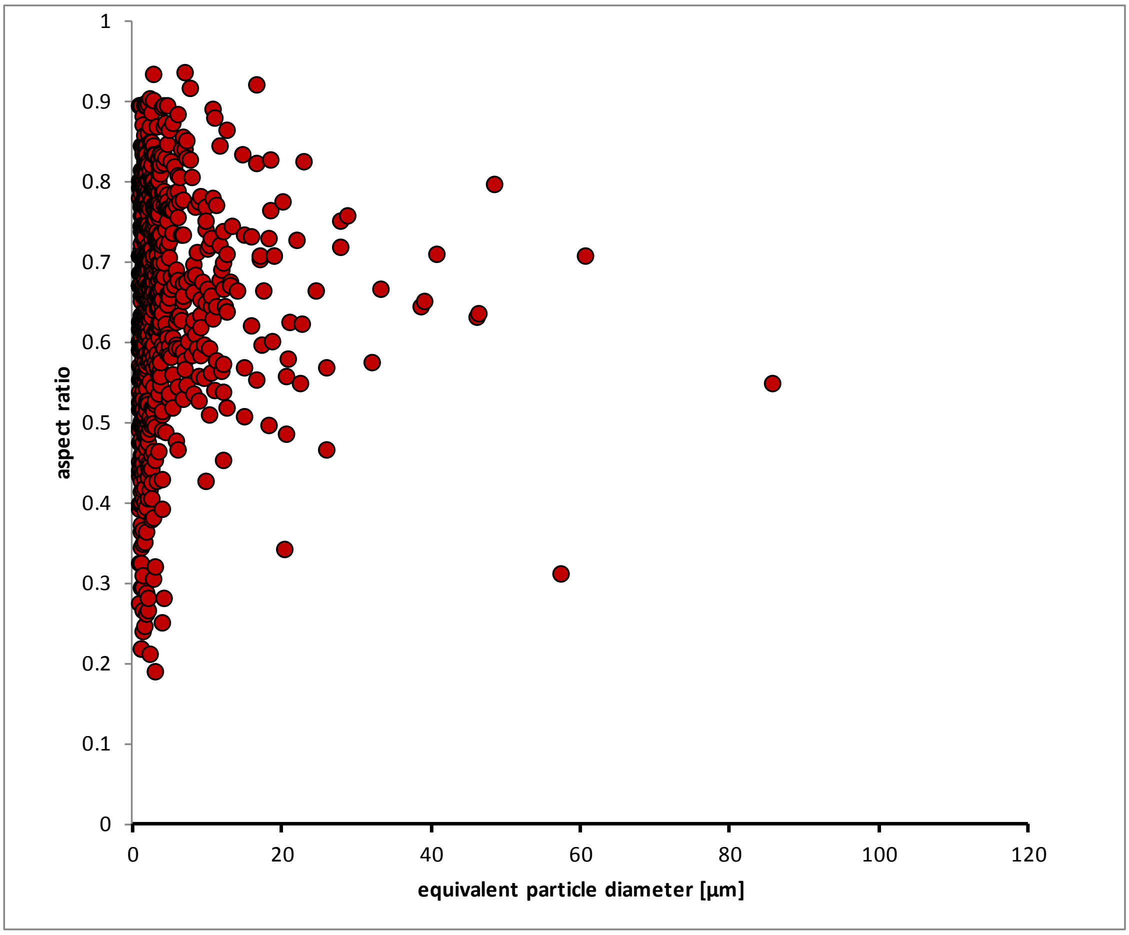

Figure 32: Aspect ratio of particles generated at 160 N/27.5 HZ (A3 pebble)

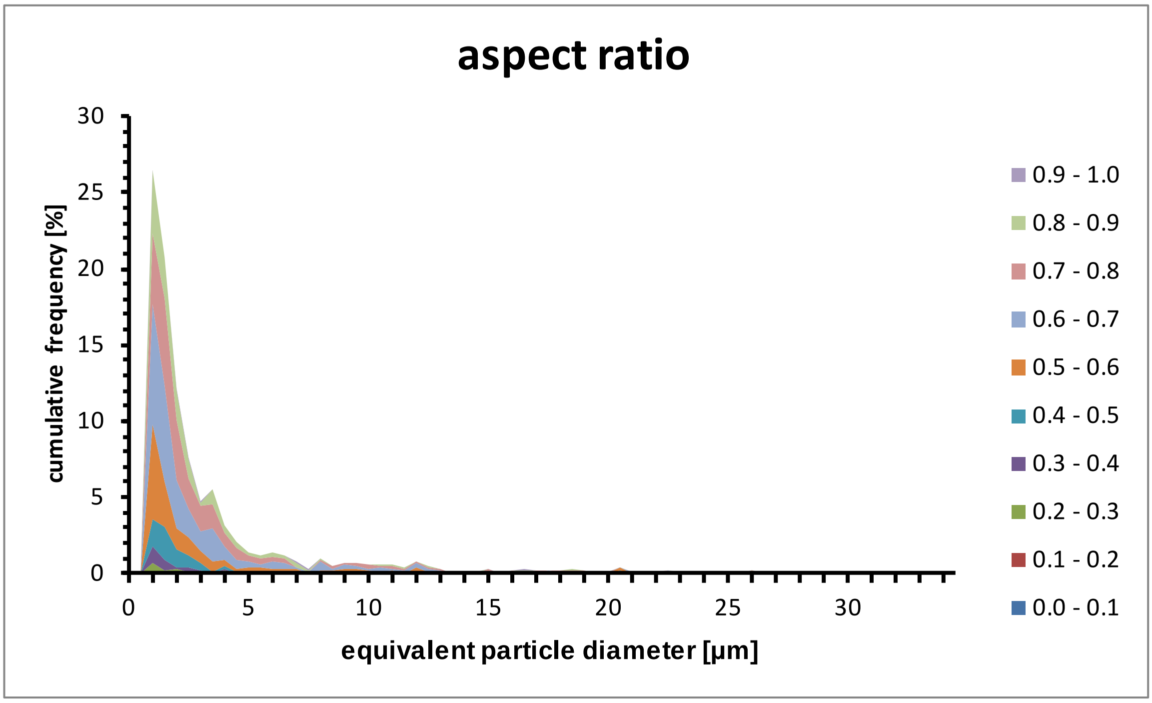

Figure 33: Distribution of the aspect ratio of particles generated at 160 N/27.5 Hz (A3 pebble)

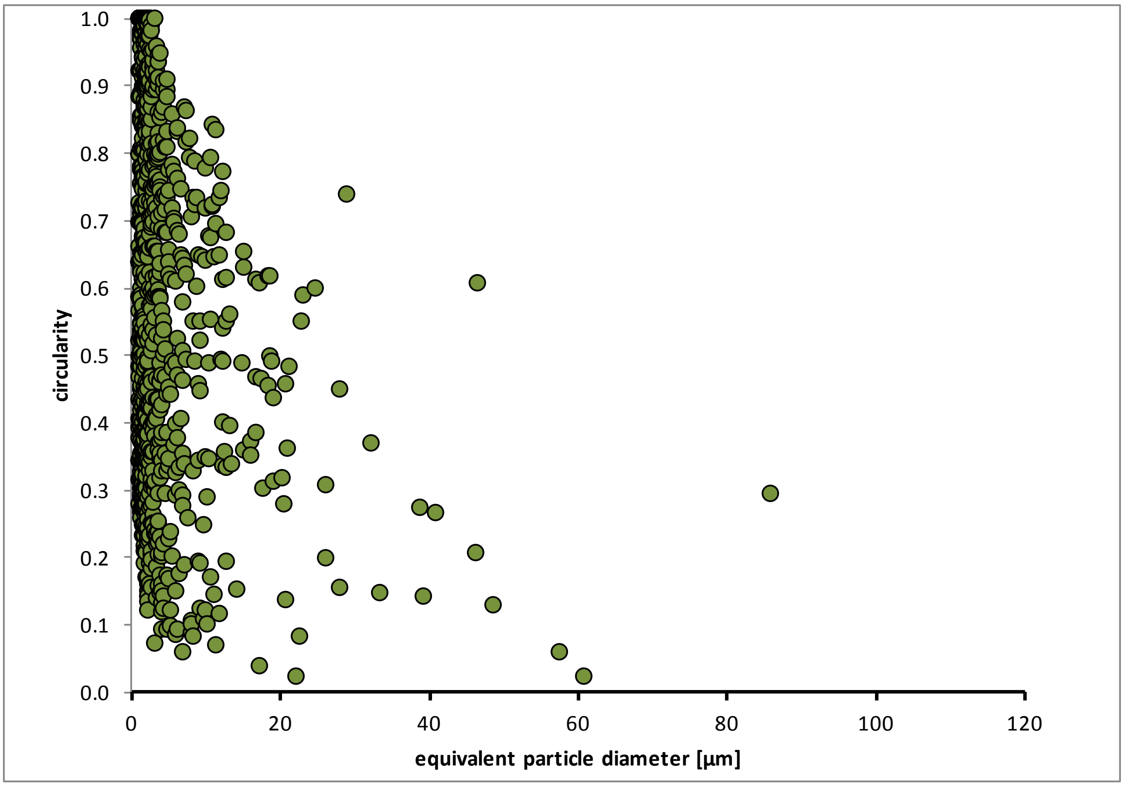

Figure 34: Overview of size and circularity of the particles under investigation (160 N/27.5 Hz, A3 pebble)

3.3 Load of 320 N at 27.5 Hz rotational frequency (A3 pebble)

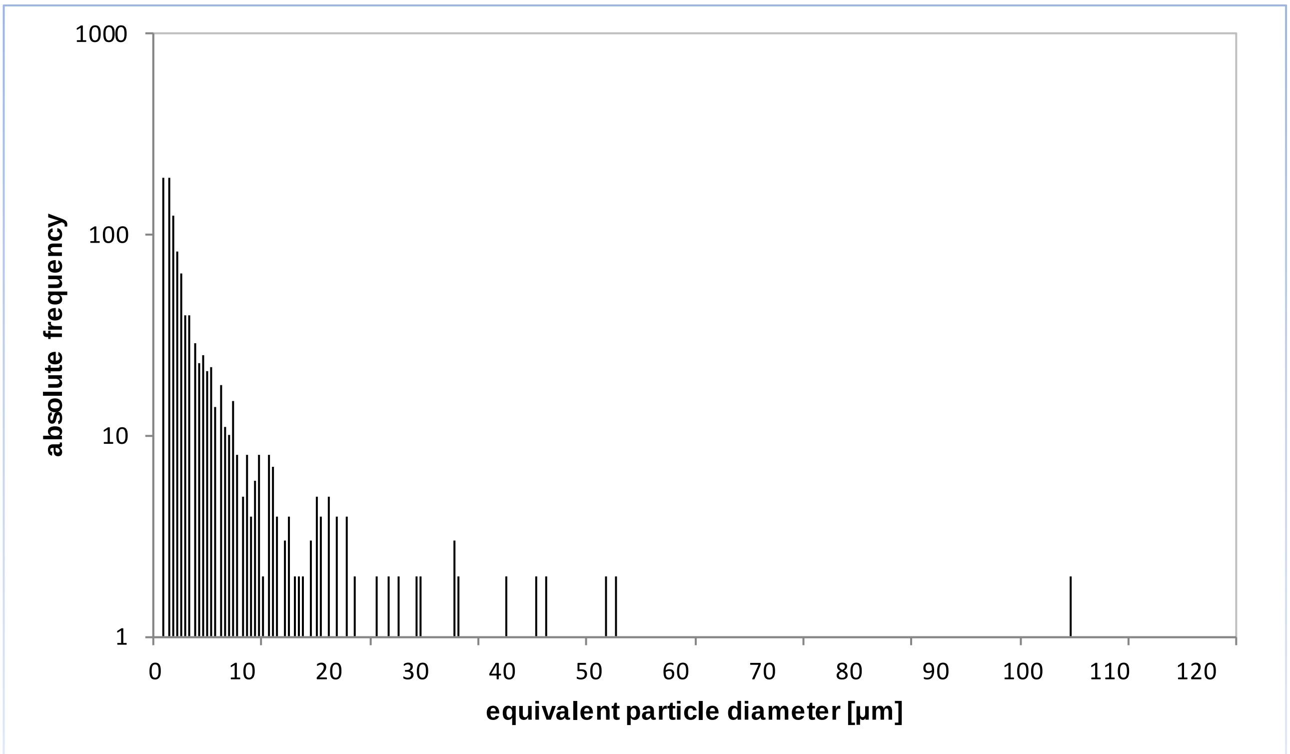

Figure 35: Particle size distribution of particles generated at 320 N /27.5 Hz (A3 pebble)

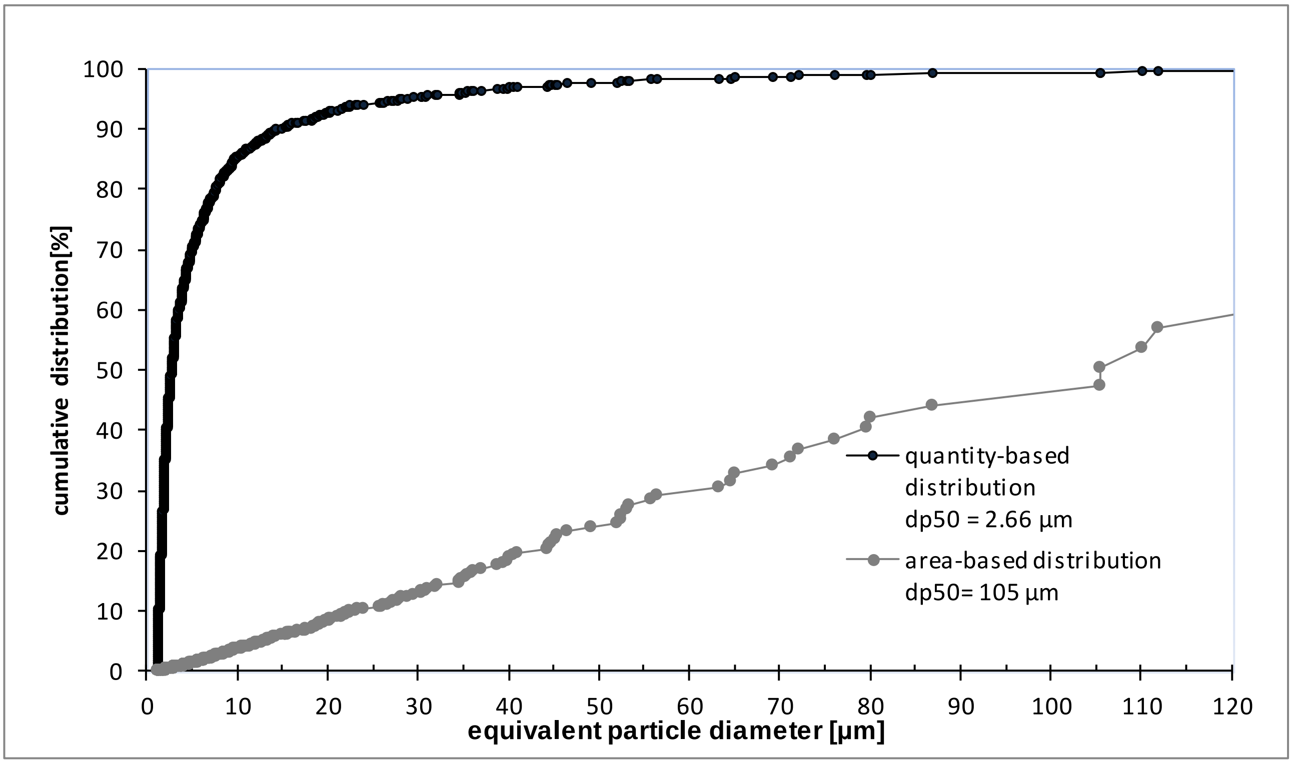

Figure 36: Cumulative particle size distribution of particles generated at 320 N/27.5 Hz (A3 pebble)

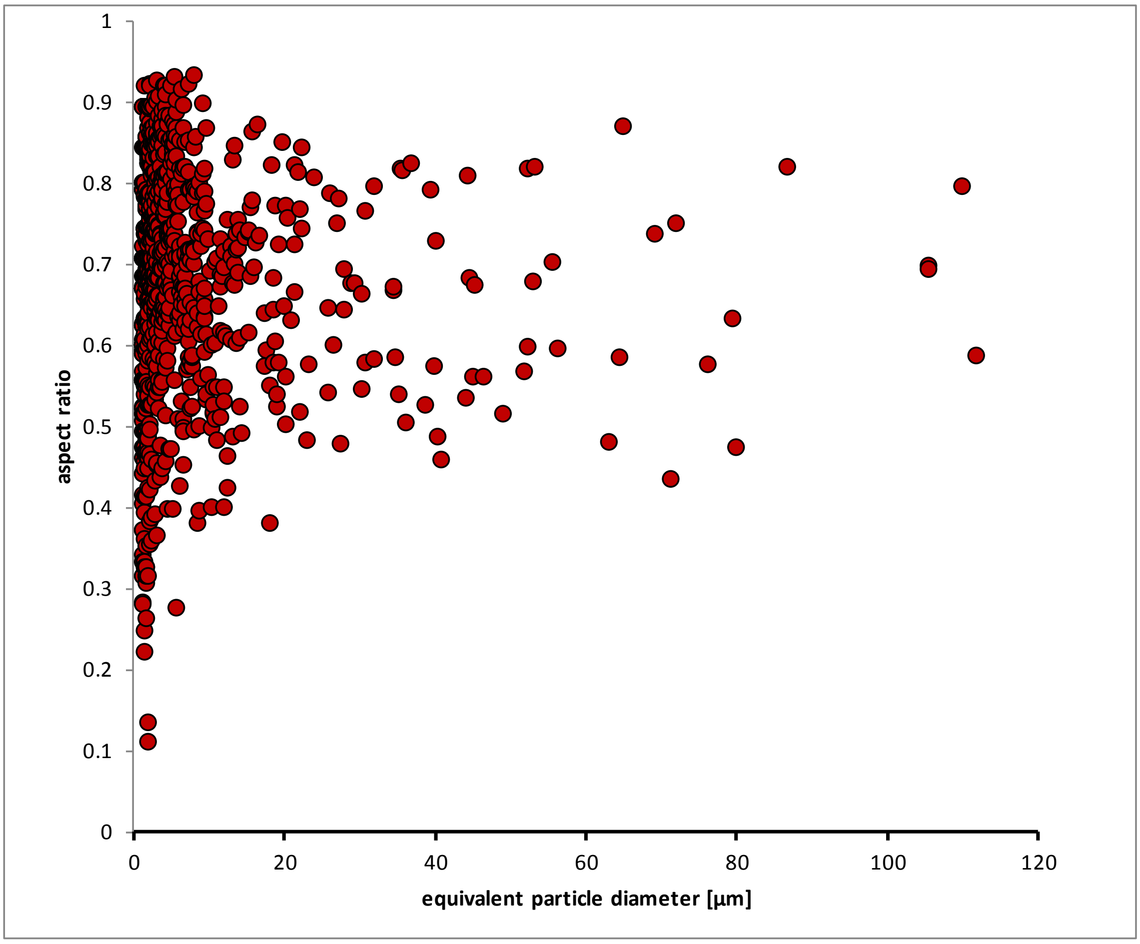

Figure 37: Aspect ratio of particles generated at 320 N/27.5 HZ (A3 pebble)

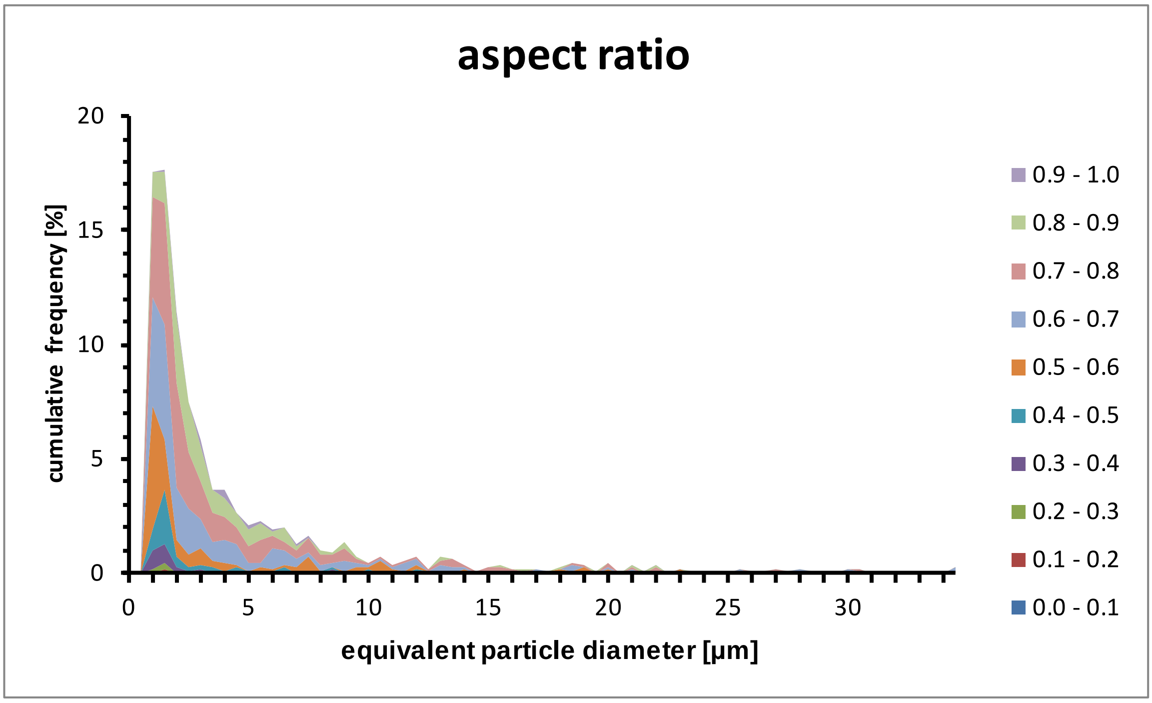

Figure 38: Distribution of the aspect ratio of particles generated at 320 N/27.5 Hz (A3 pebble)

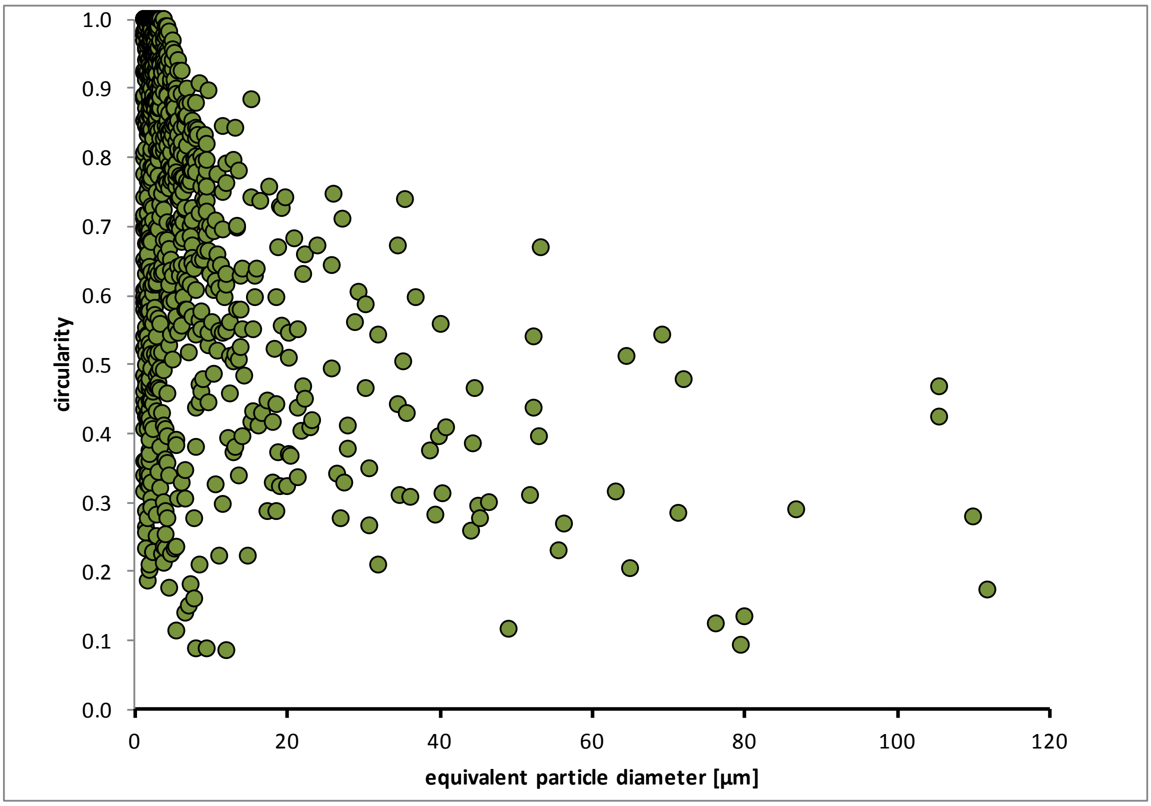

Figure 39: Overview of size and circularity of the particles under investigation (320 N/27.5 Hz, A3 pebble)

3.4 Load of 640 N at 27.5 Hz rotational frequency (A3 pebble)

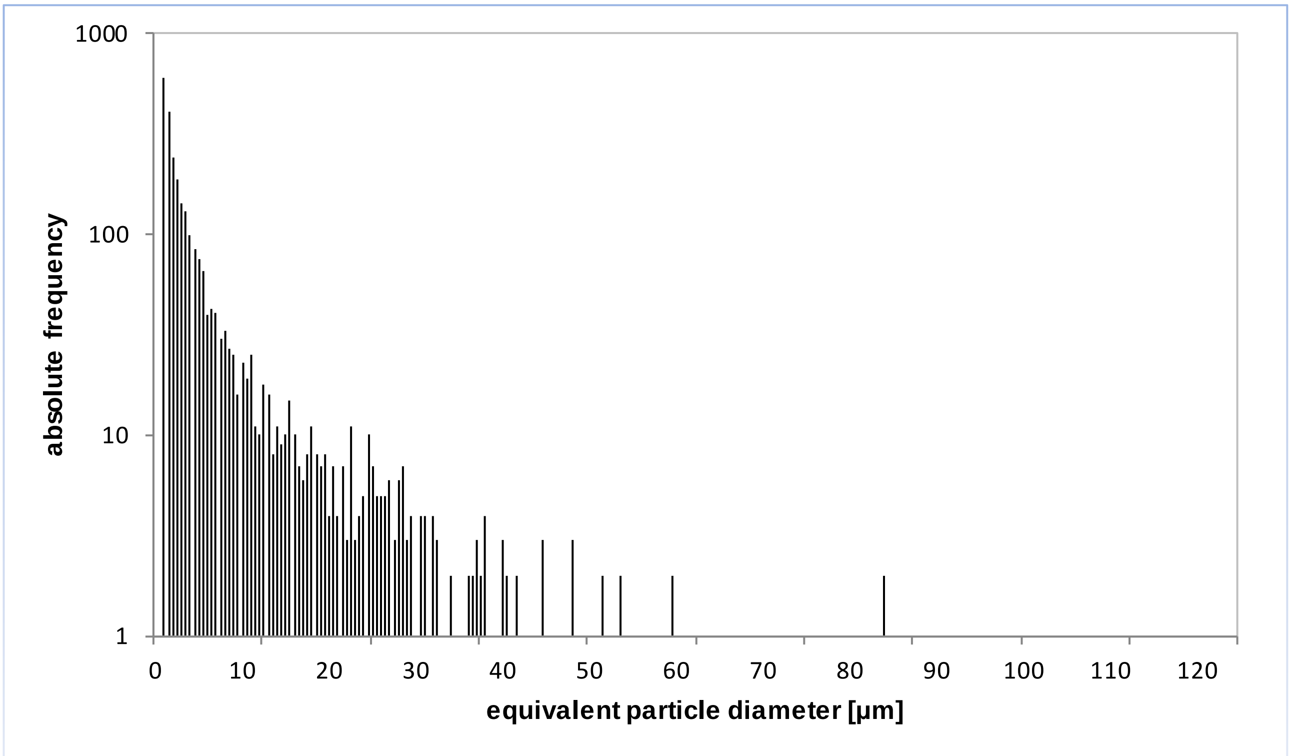

Figure 40: Particle size distribution of particles generated at 640 N /27.5 Hz (A3 pebble)

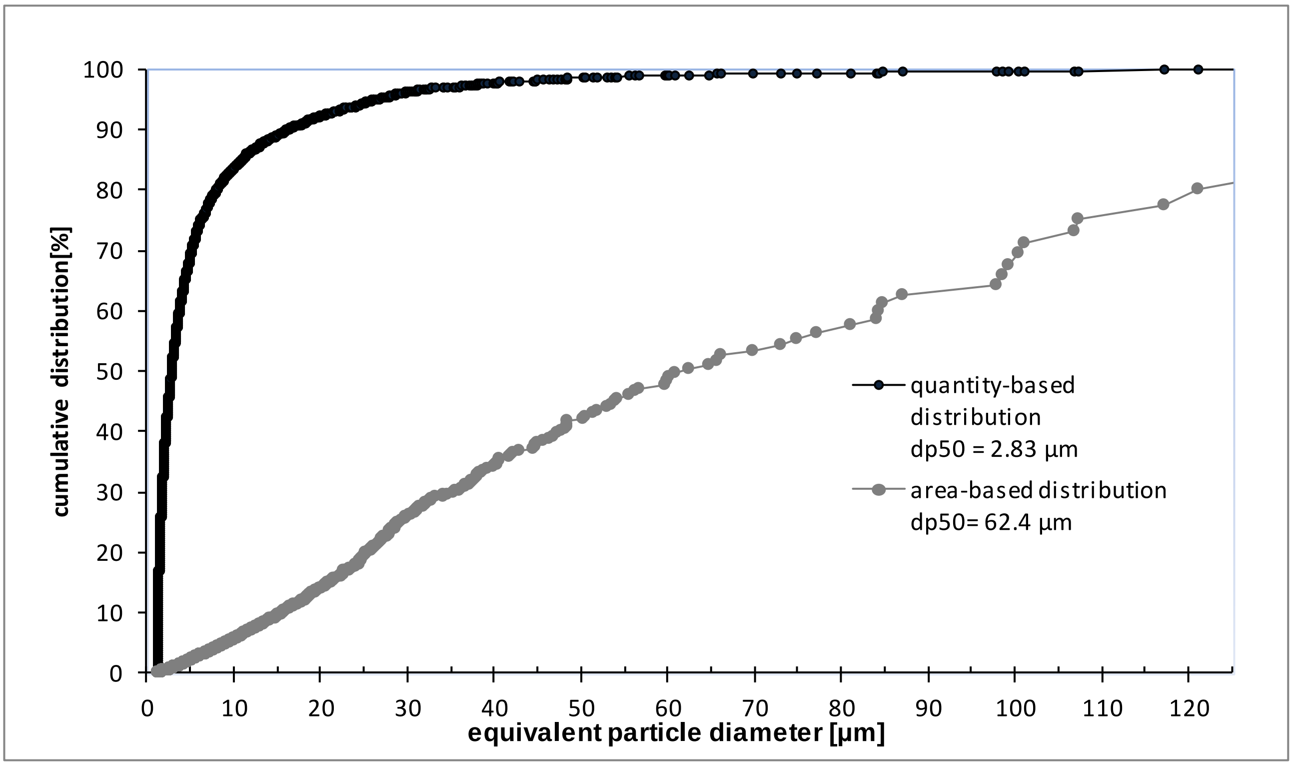

Figure 41: Cumulative particle size distribution of particles generated at 640 N/27.5 Hz (A3 pebble)

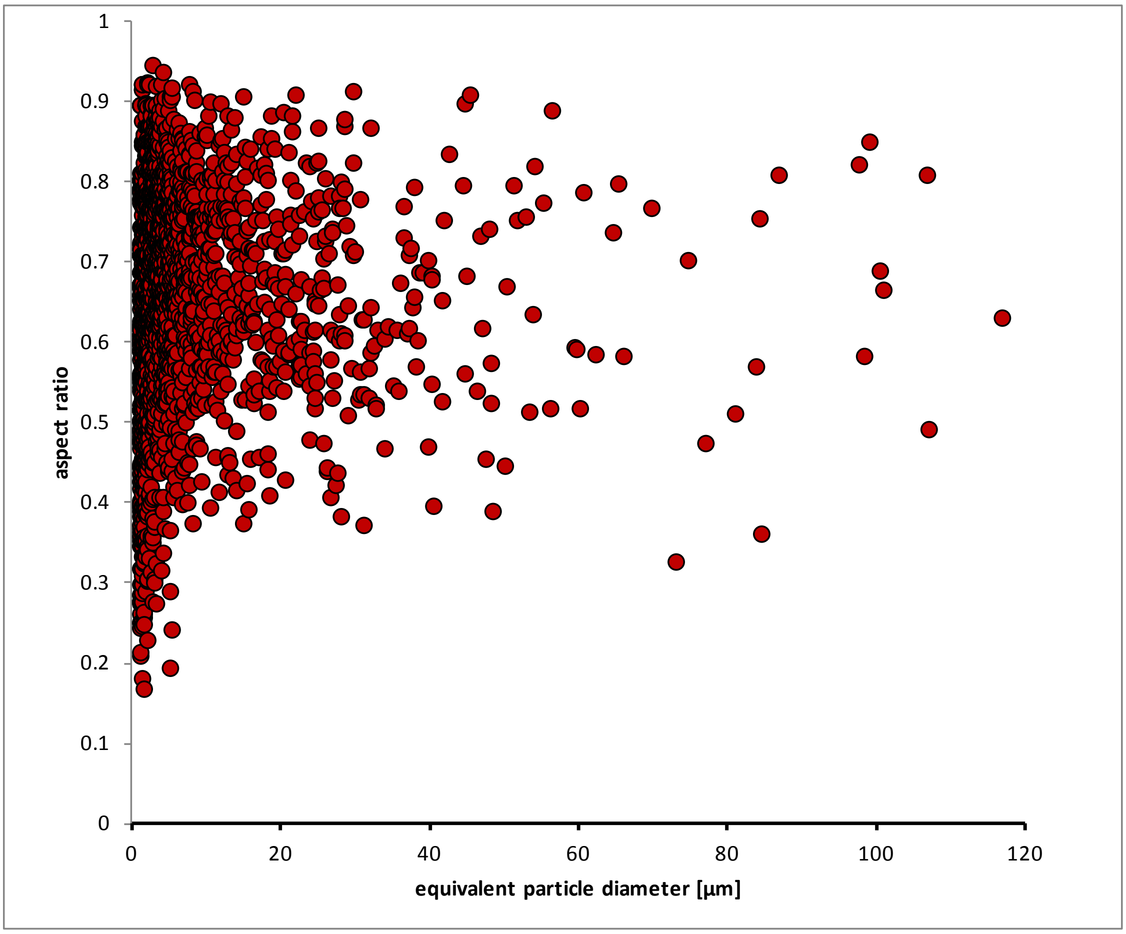

Figure 42: Aspect ratio of particles generated at 640 N/27.5 HZ (A3 pebble)

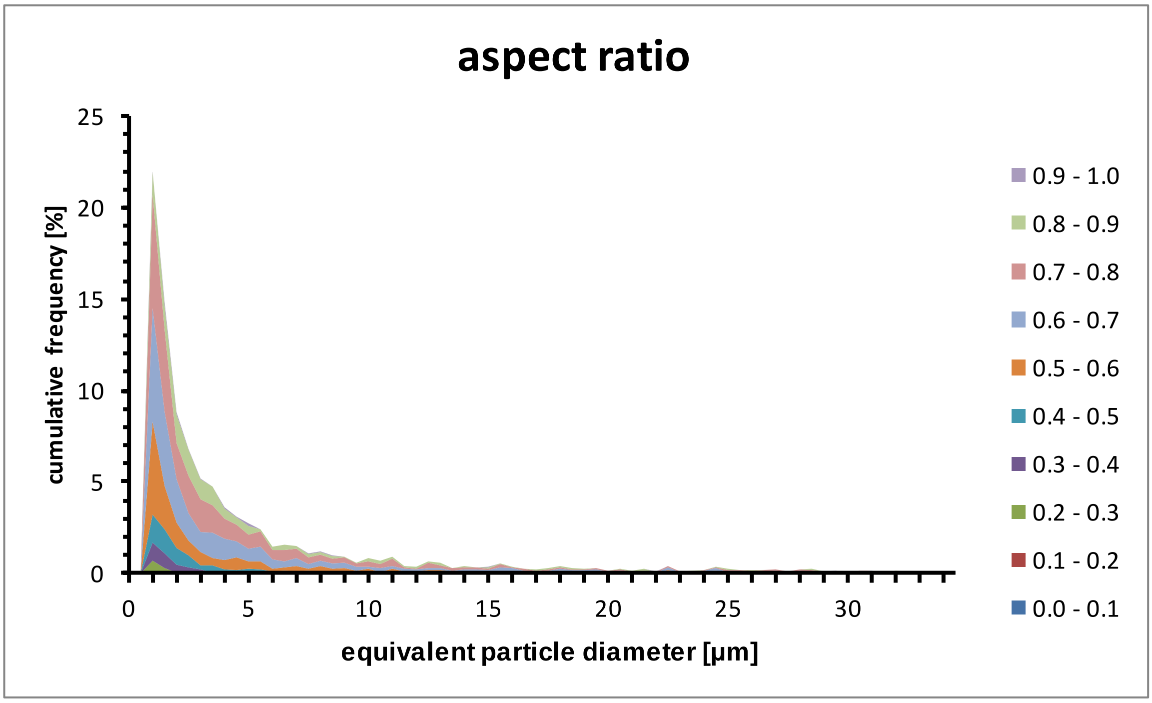

Figure 43: Distribution of the aspect ratio of particles generated at 640 N/27.5 Hz (A3 pebble)

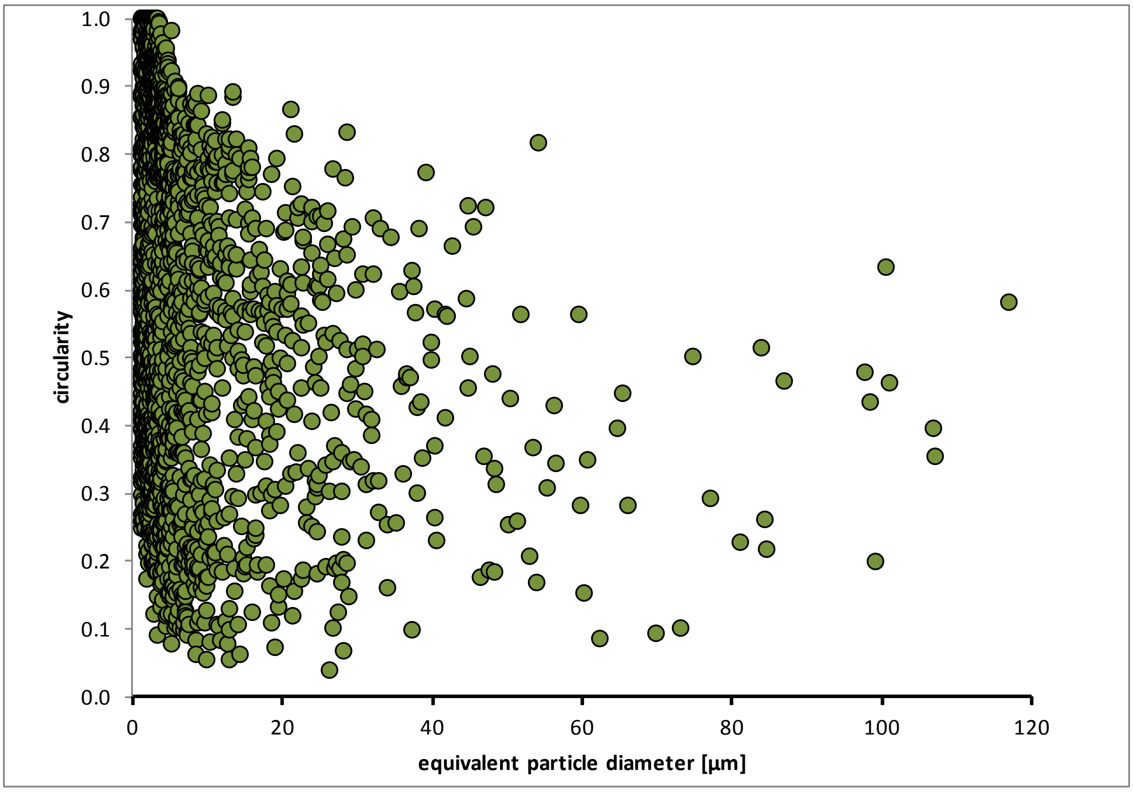

Figure 44: Overview of size and circularity of the particles under investigation (640 N/27.5 Hz, A3 pebble)

4 Results of A3 pebble against reflector disc friction experiments

Friction experiments were carried out in the p-w configuration, i.e. compared to the prior experiments, the lower 3 half pebbles along with the center pebble were replaced by a NBG-17 graphite disc. These experiments should represent the case in which, in the reactor core, the outermost pebbles grind on the reflector walls.

In the p-w experiment with a contact force of 160 N, only a few large particles were generated, significantly less than in the p-p-p experiment with a contact force of 160 N using A3 pebbles. However, the number-weighted particle diameter was a bit larger than in the p-p-p experiment, whereas the area-weighted diameter was substantially lower (Table 3)

Table 3: Comparison of p-p-p and p-w experiments using A3 pebbles and, in the p-w configuration, a NBG-17 graphite disc at 160 N contact load

graphite grade	diameter	Friction against NBG-17 graphite disc (p-w)	Pebble-pebble friction (p-p-p)
A3	d_{p50} (quantity)	3.04	2.13
	d_{p50} (area)	18.6	28.0

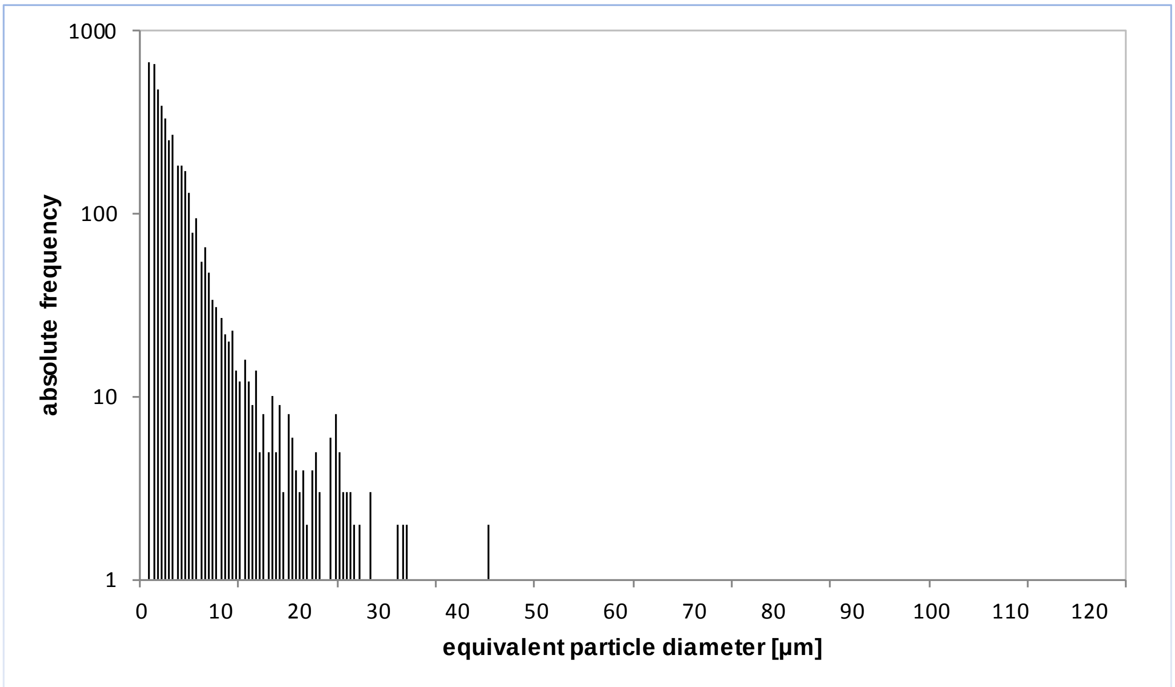

Figure 45: Particle size distribution of particles generated at 160 N Hz (A3 pebble against NBG-17 disc)

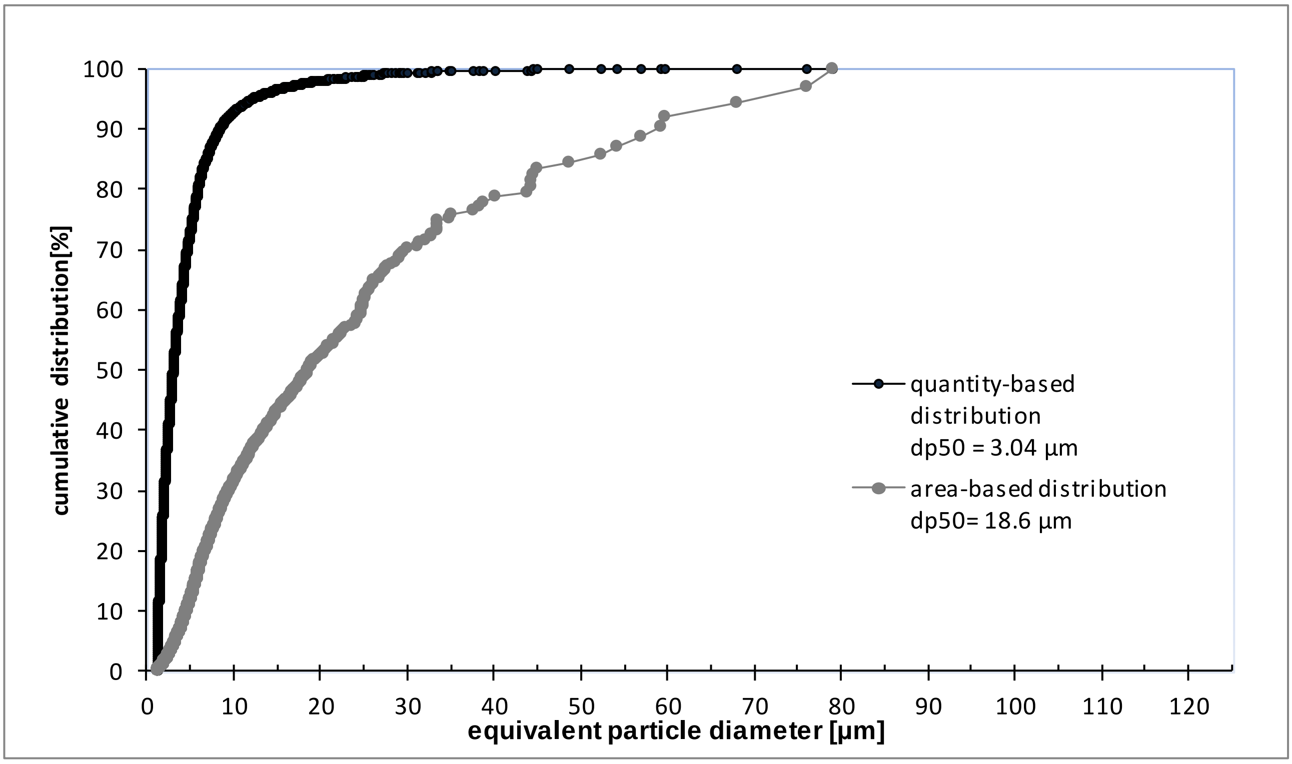

Figure 46: Cumulative particle size distribution of particles generated at 160 N/27.5 Hz (A3 pebble against NBG-17 disc)

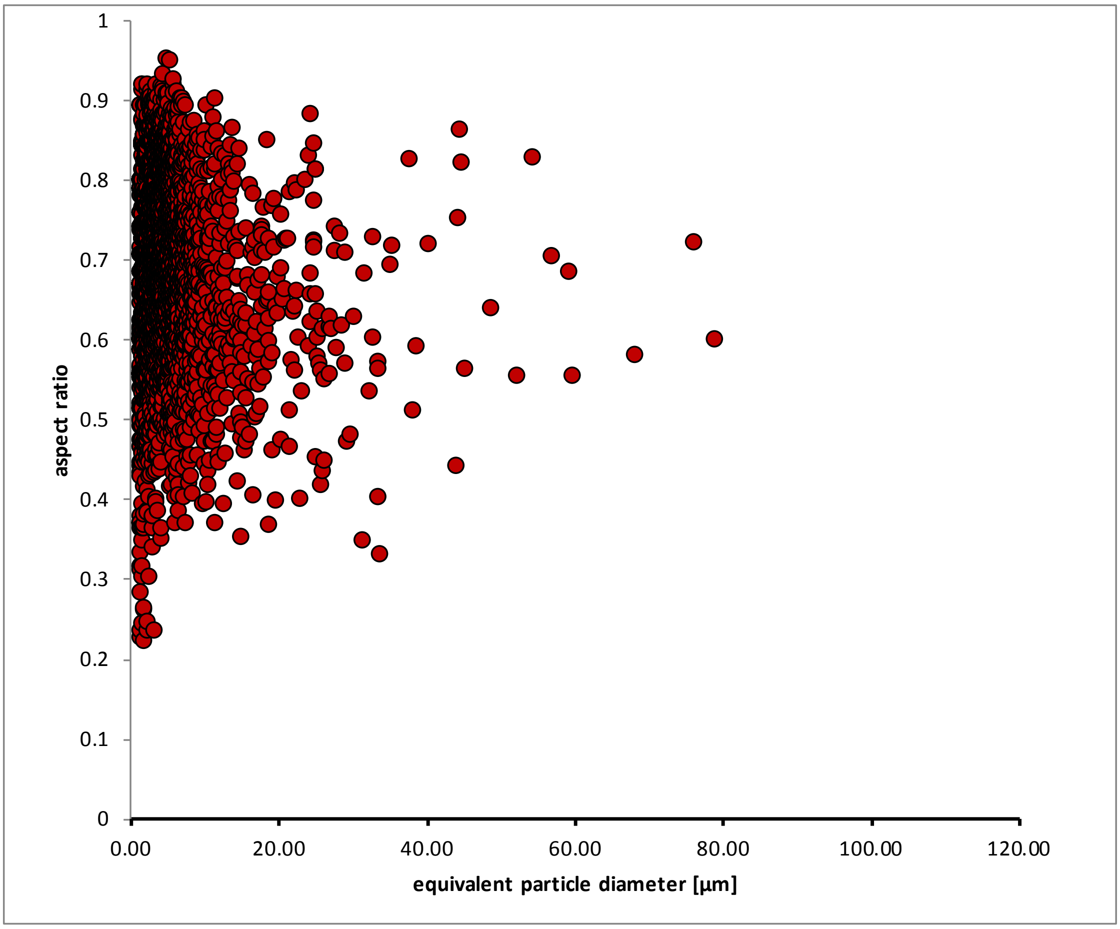

Figure 47: Aspect ratio of particles generated at 160 N/27.5 Hz (A3 pebble against NBG-17 disc)

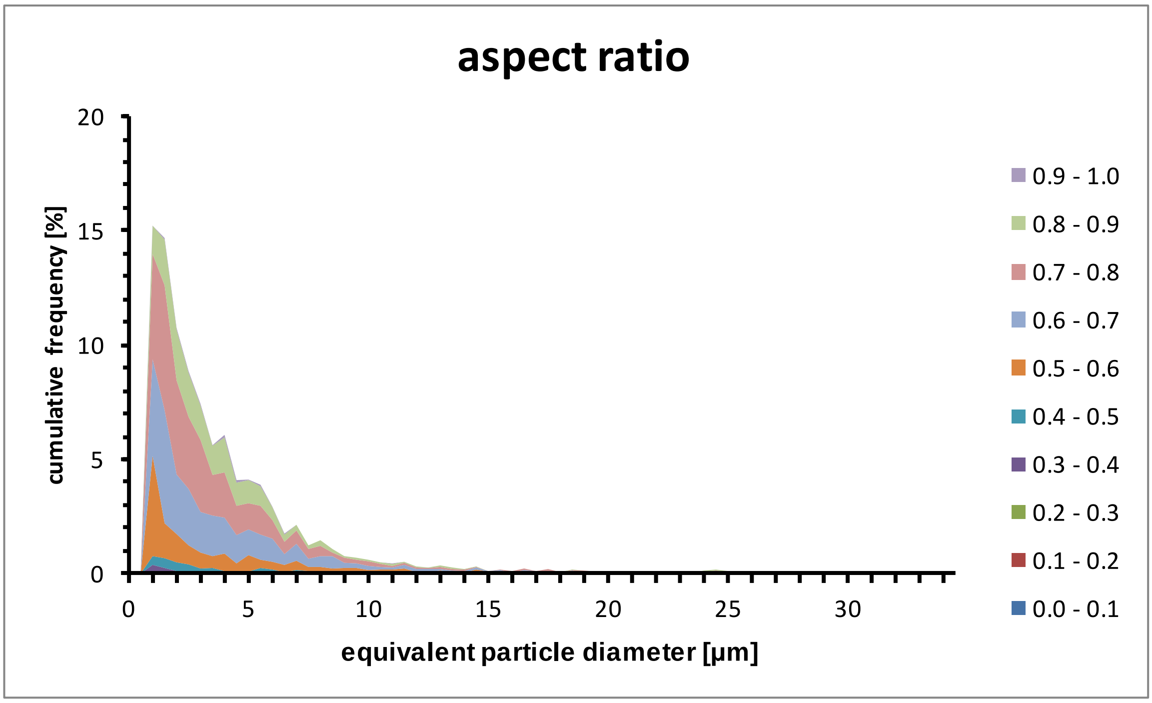

Figure 48: Distribution of the aspect ratio of particles (A3 pebble against NBG-17 disc)

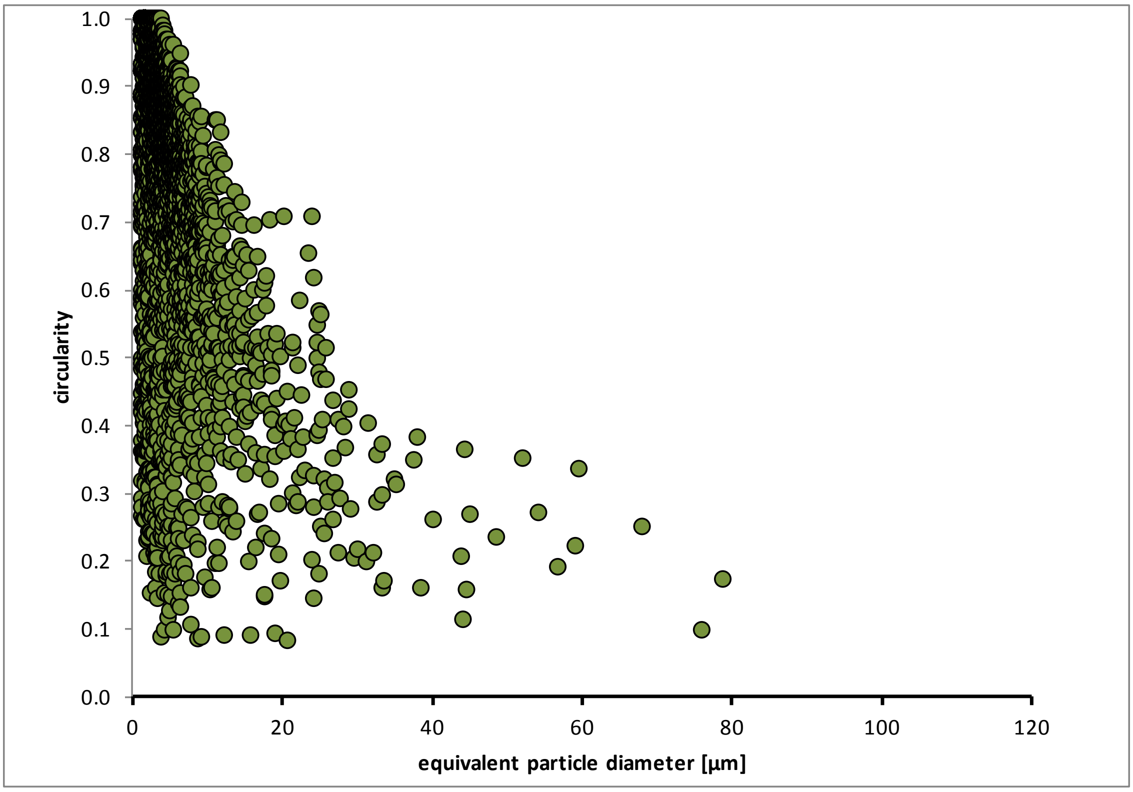

Figure 49: Overview of size and circularity of the particles under investigation (A3 pebble against NBG-17 disc)

5 Results of p-p-p friction experiments with continuously increasing contact force

In order to reproduce the pebble movement from the top to the bottom of the pebble bed as close as possible experimentally, the load of the pebbles was continuously increased from 80 N to 640 N in steps of 80 N. It was expected that most particles would be generated at the highest load. Indeed, results with respect to amount and size distribution of generated particles were similar to those obtained at constant load of 320 N and 640 N both for MLRF and A3 pebbles (Table 3).

Table 4: Comparison of the results for constant and continosly increasing load

graphite grade	diameter	Continuously increasing load (80-640 N)	Constant load (320 N and 640 N)
MLRF	d_{p50} (quantity) d_{p50} (area)	2.66 28.2	2,52 – 3.14 33.2 - 48.3
A3	d_{p50} (quantity) d_{p50} (area)	2.91 104.6	2.66 - 2.83 62.4 - 106.0

5.1 Results for continuously increasing load (MLRF pebbles)

The evaluation of particles generated by abrasion of graphite pebbles under continuously increasing load were performed in the same manner as described for particles generated by abrasion of graphite pebbles under constant load described in chapter 2. For each experimental run, discrete and cumulative particle size distributions were determined (the first and second figure, respectively) as well as the particle aspect ratio (third and fourth figure, respectively), and the particle circularity (fifth figure).

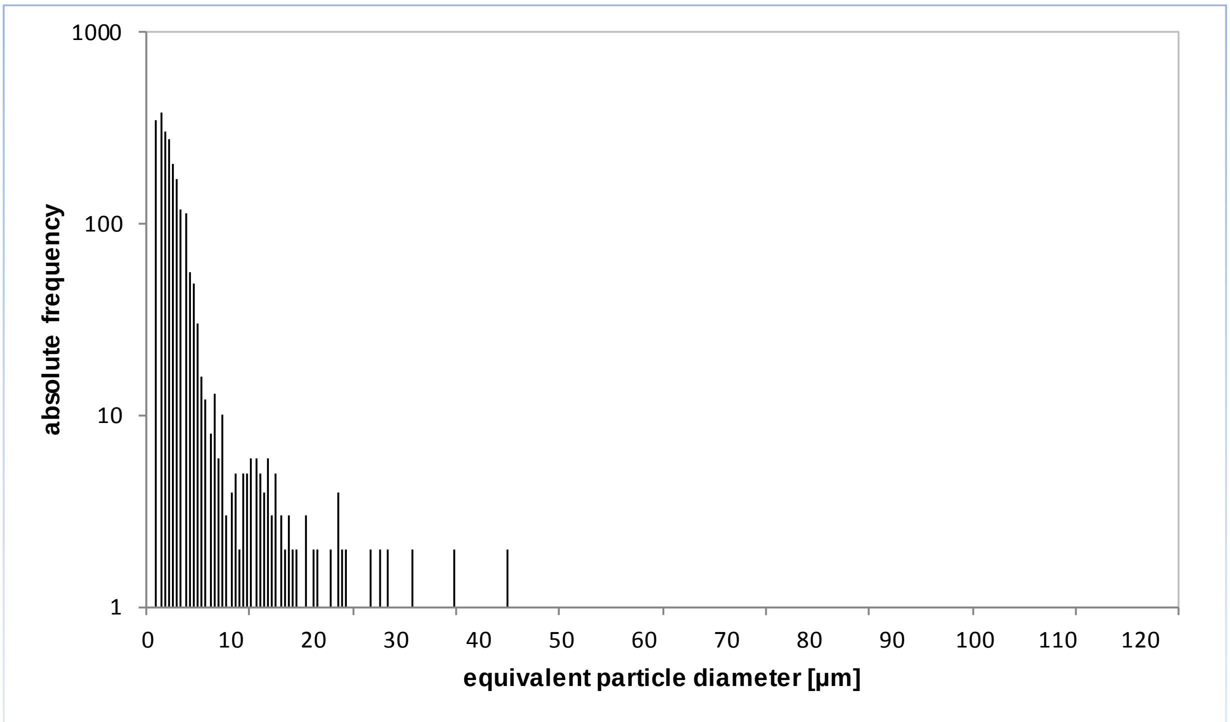

Figure 50: Particle size distribution of particles generated at a continuously increasing load of 80 – 640 N at 27.5 Hz (MLRF pebble)

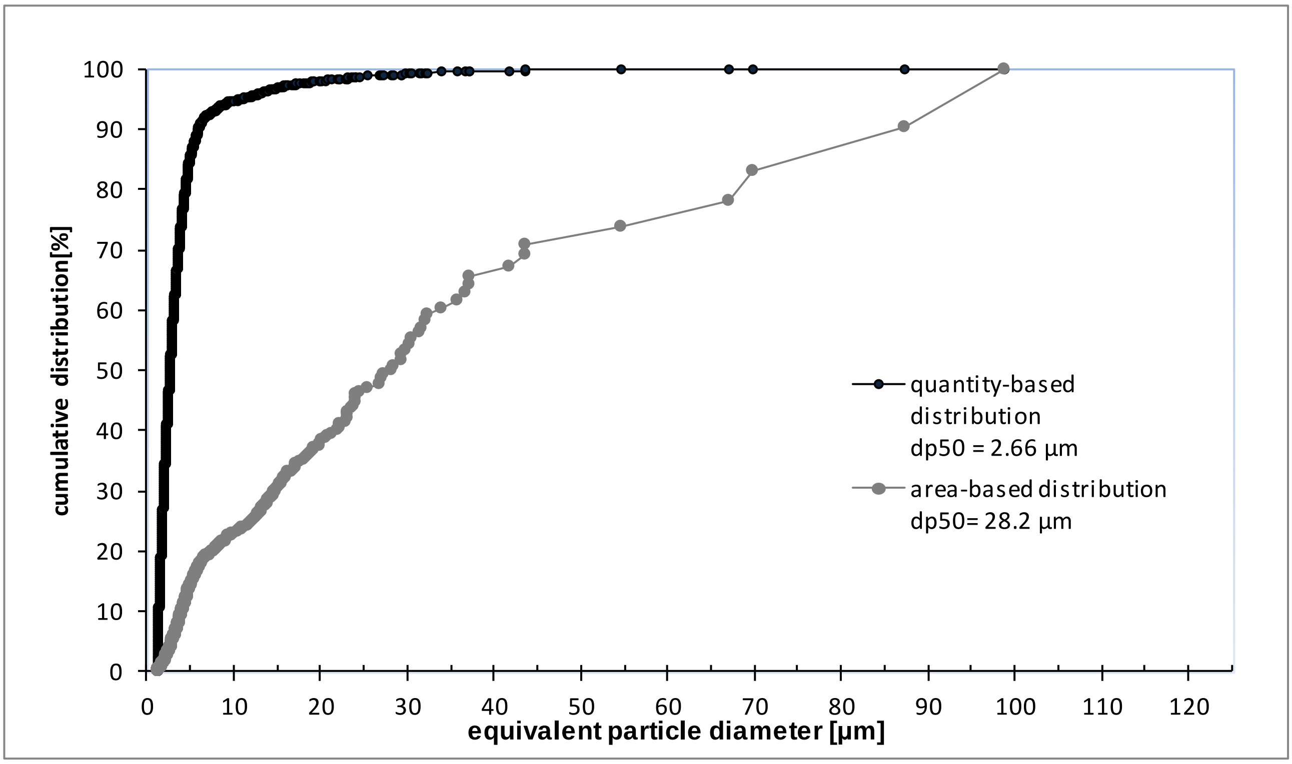

Figure 51: Cumulative particle size distribution of particles generated at a continuously increasing load of 80 – 640 N at 27.5 Hz (MLRF pebble)

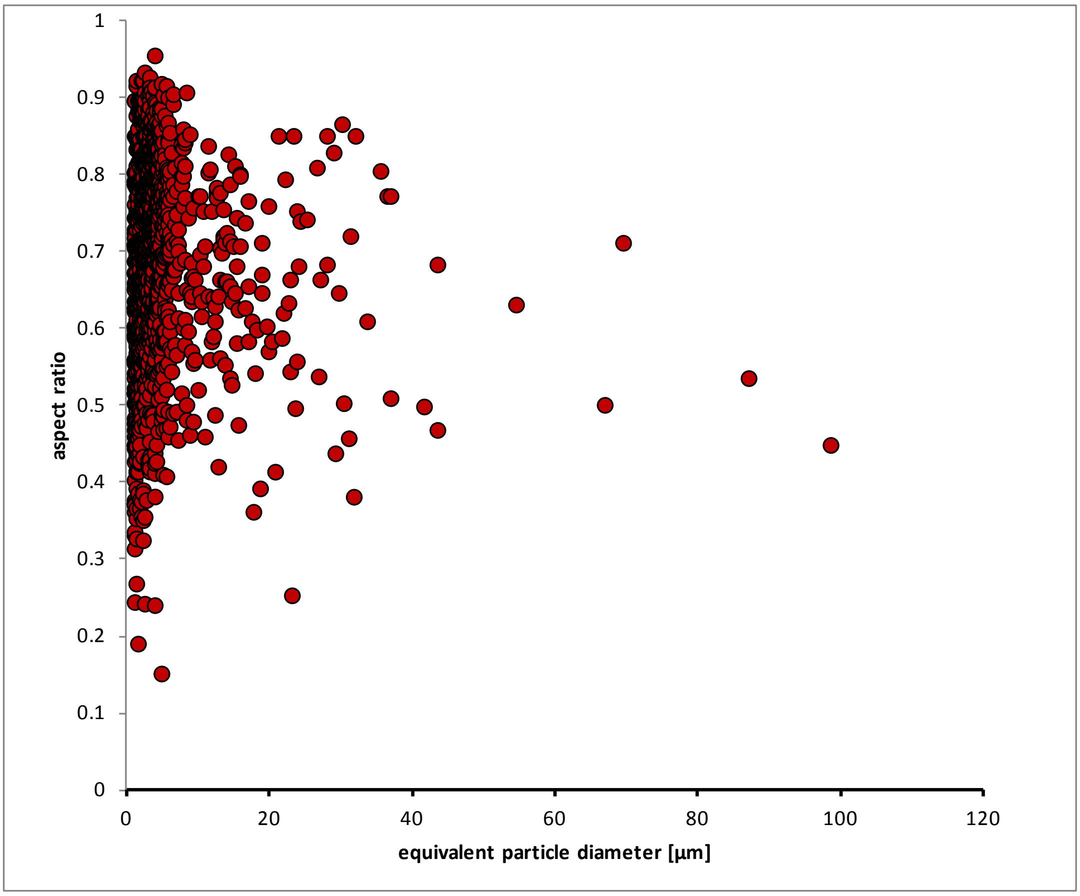

Figure 52: Aspect ratio of particles generated at a continuously increasing load of 80 – 640 N at 27.5 Hz (MLRF pebble)

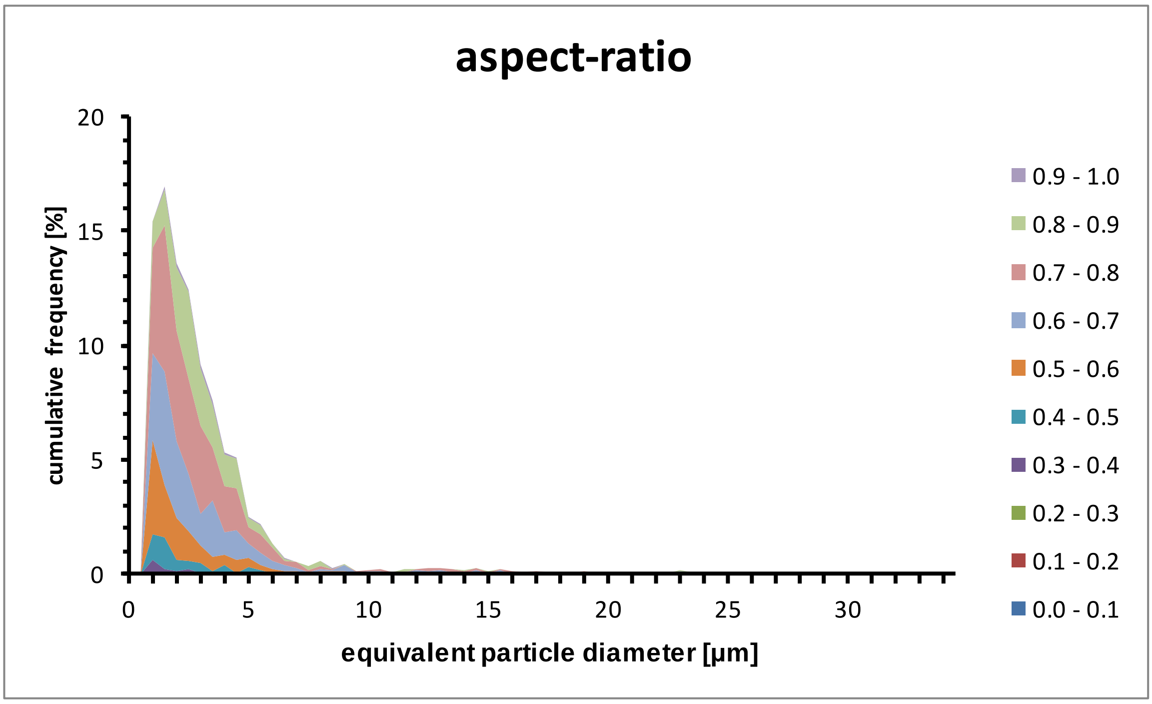

Figure 53: Distribution of the aspect ratio of particles generated at a continuously increasing load of 80 – 640 N at 27.5 Hz (MLRF pebble)

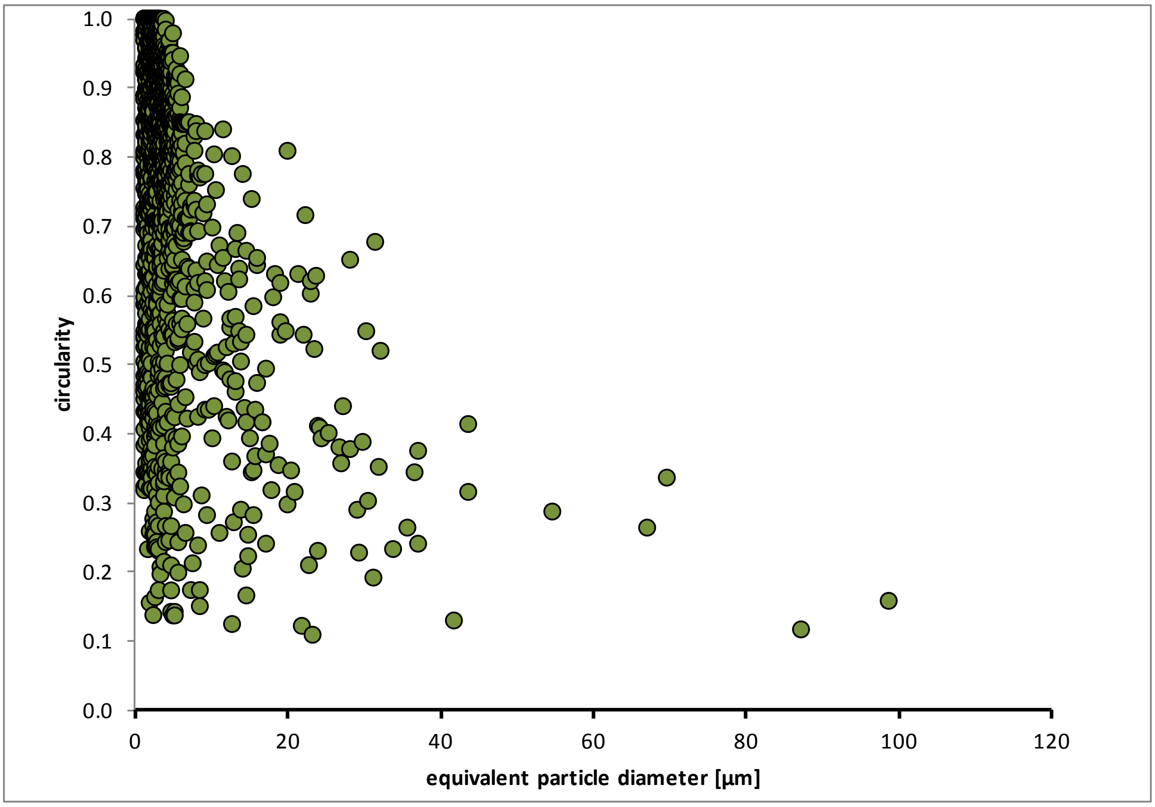

Figure 54: Overview of size and circularity of the particles under investigation at a continuously increasing load of 80 – 640 N at 27.5 Hz (MLRF pebble)

5.2 Results for continuously increasing load (A3 pebbles)

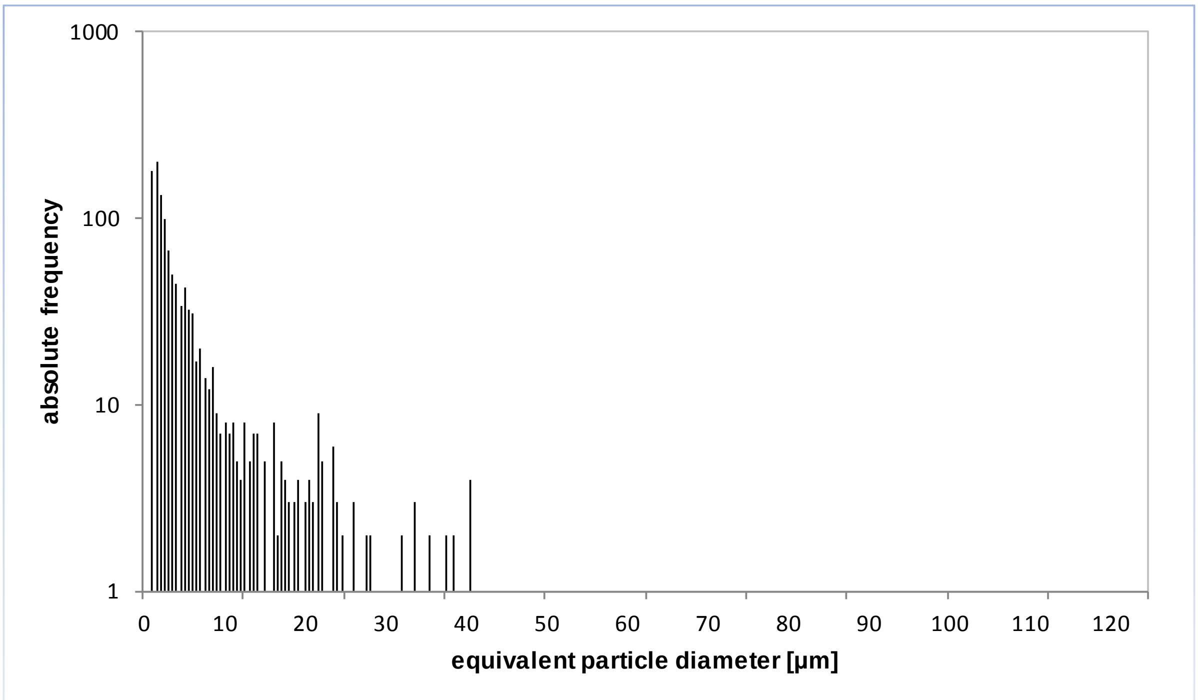

Figure 55: Particle size distribution of particles generated at a continuously increasing load of 80 – 640 N at 27.5 Hz (A3 pebble)

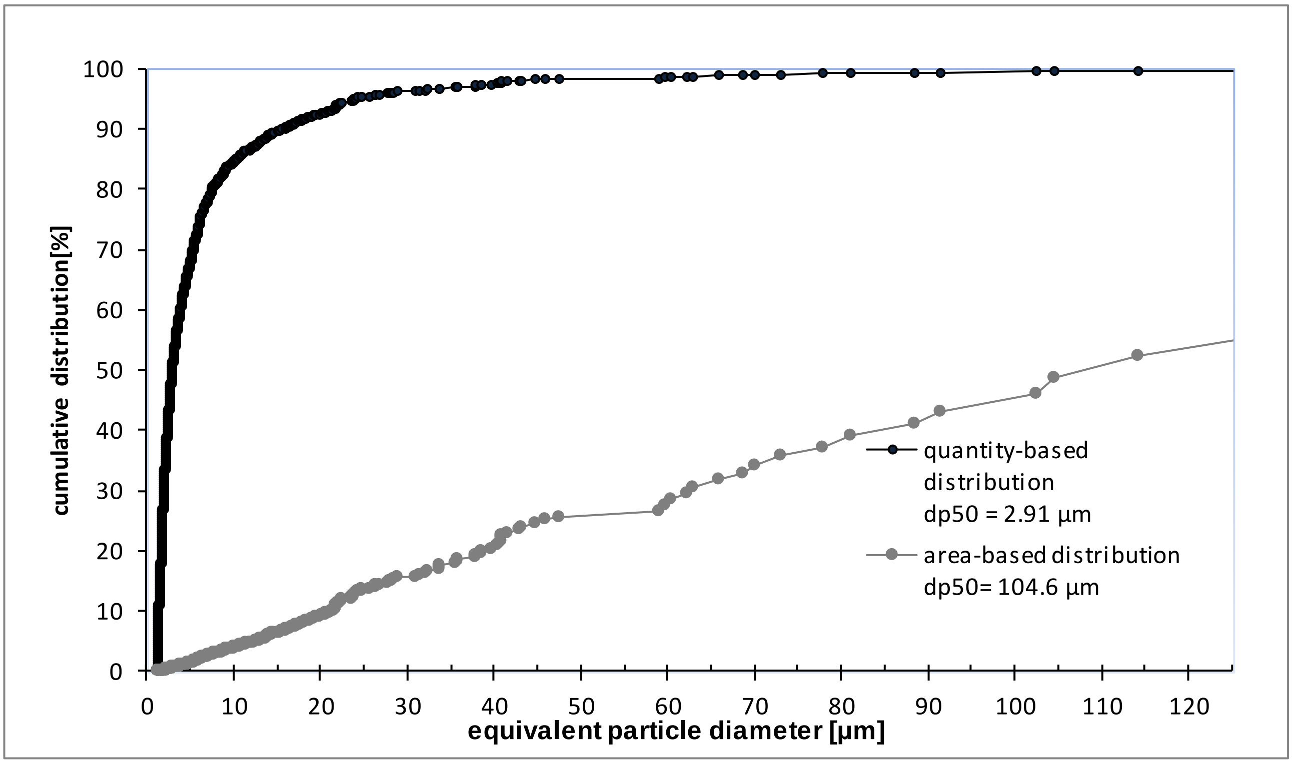

Figure 56: Cumulative particle size distribution of particles generated at a continuously increasing load of 80 – 640 N at 27.5 Hz (A3 pebble)

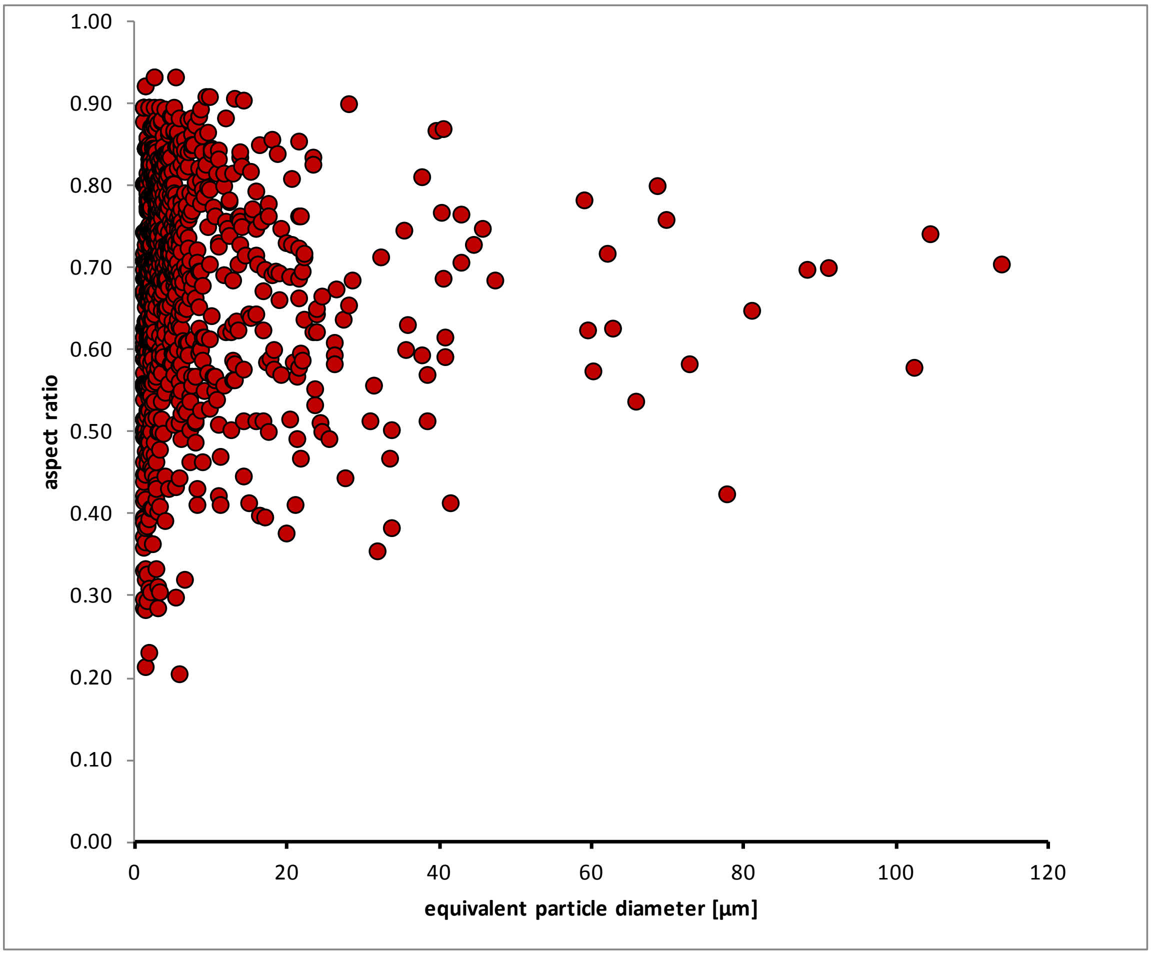

Figure 57: Aspect ratio of particles generated at a continuously increasing load of 80 – 640 N at 27.5 Hz (A3 pebble)

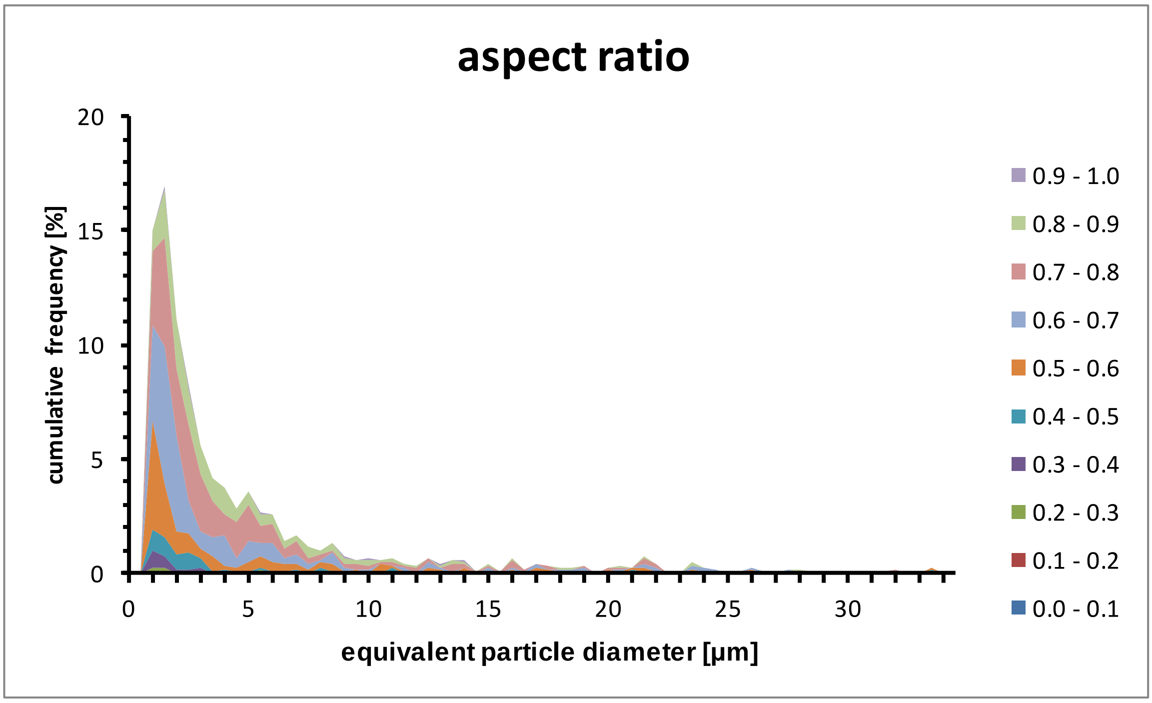

Figure 58: Distribution of the aspect ratio of particles generated at a continuously increasing load of 80 – 640 N at 27.5 Hz (A3 pebble)

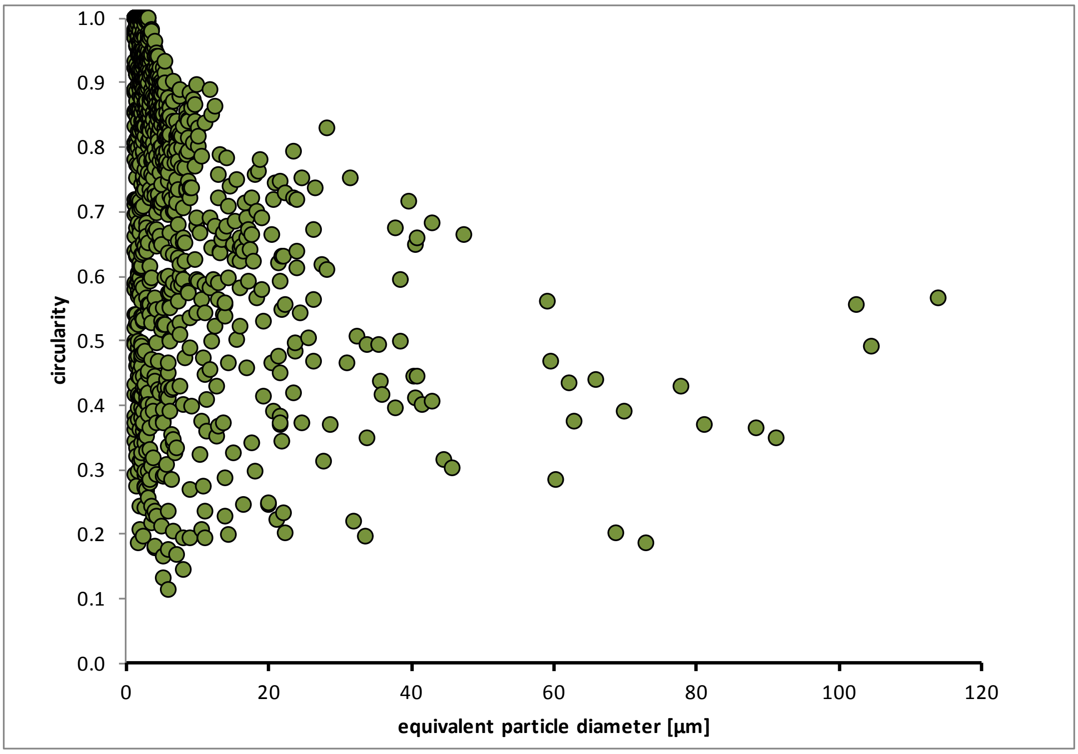

Figure 59: Overview of size and circularity of the particles under investigation at a continuously increasing load of 80 – 640 N at 27.5 Hz (A3 pebble)

6 Comprehensive comparison and discussion of the results obtained in the friction experiments

6.1 Comparison of the cumulative particle size distributions of particles obtained by friction of A3 pebbles

Due to experimental limitations of the test facility such as impure helium atmosphere and an operation temperature close to room temperature, the particle size distributions determined in this work cannot be understood as representative for graphite particles generated in a HTR core. However, some clear trends were observed that should also be relevant for HTR conditions. Most significantly, the particle size distribution shifted to larger values if the contact force was increased. Accordingly, it can be expected that the deeper a pebble is positioned in the pebble bed, the larger the generated particles will be. Based on their number, most particles exhibited a diameter smaller than 5 µm. At high contact forces, relatively large particles (d_p> 60 µm) were generated that skewed the area-weighted size distribution to higher values for the diameter. The area-weighted median diameter $d_{p,50}$ was the highest for particles obtained at medium load, where some exceptionally large particles (d_p>100 µm) were observed. The diagram for the different loads can be seen in figure 60.

6.2 Comparison of the aspect ratio of particles obtained by friction of A3 pebbles

For all particles under investigation the aspect ratio ($Ferret_{min}/Ferret_{max}$) was between 0.3 and 0.9 irrespective of the applied load. Accordingly, although particles were non-spherical, they were not rod-shaped either. Most particles had aspect ratios between 0.5 and 0.8. Based on these results it should be possible to use existing correlations for spherical particles for characterization of the transport behavior of these non-spherical particles if shape factors are taken into account. However, determination of the extent of particles in the third dimension is required for conclusive results. Based on the observed particle shapes, it can be concluded that the variation of the particle shape increases with contact load. Future work needs to determine whether this is solely a measurement artifact due to low resolution of the particle micrographs, or which effects cause this higher degree of particle uniformity. Scatter plots of the particle shape as a function of particle size for each particle is shown in figure 61 for particles that were generated under 4 different loads (80 N, 160 N, 320 N, 640 N) using load scenario ppp.

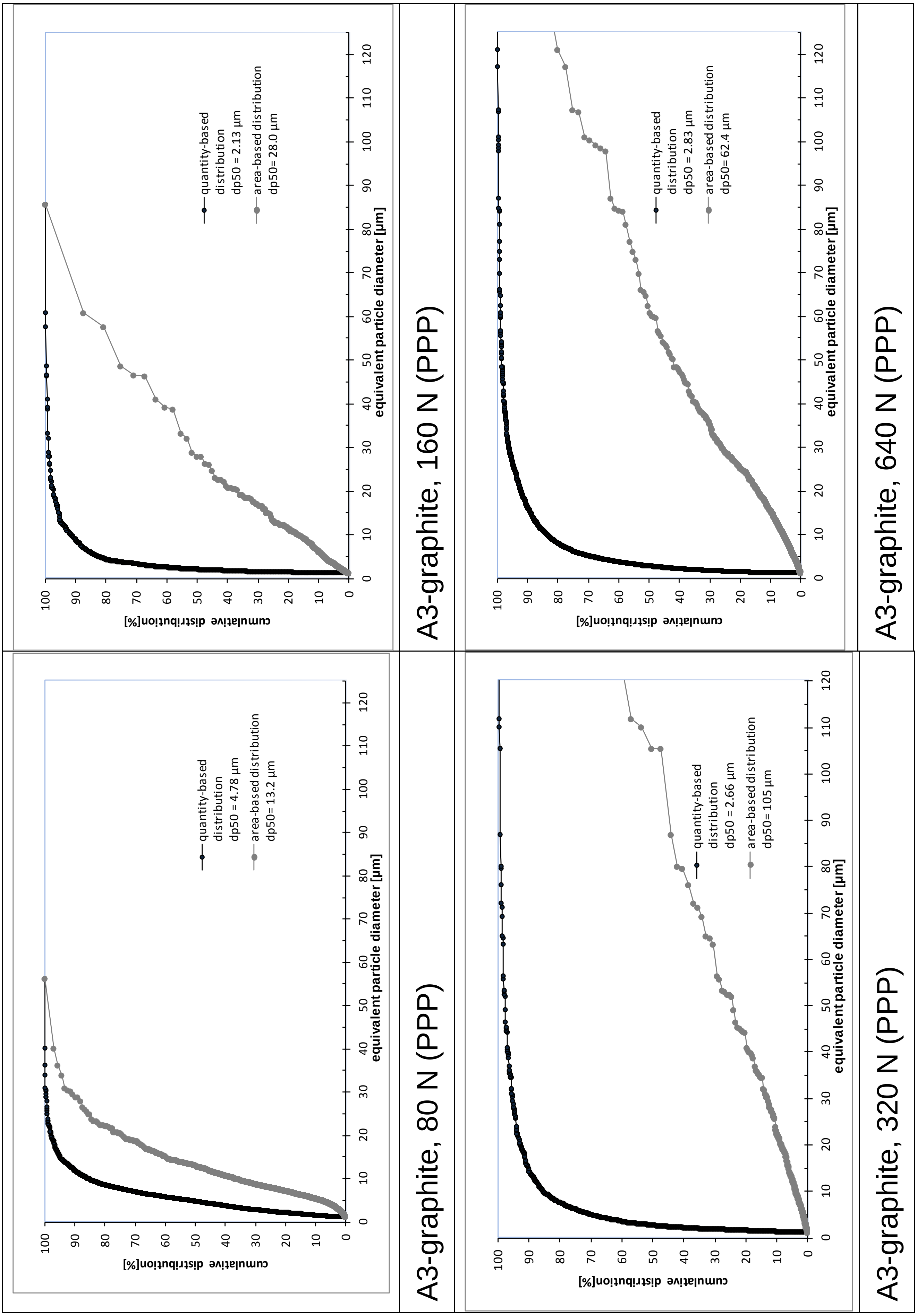

Figure 60: Comparison of cumulative particle size distribution (A3 pebble)

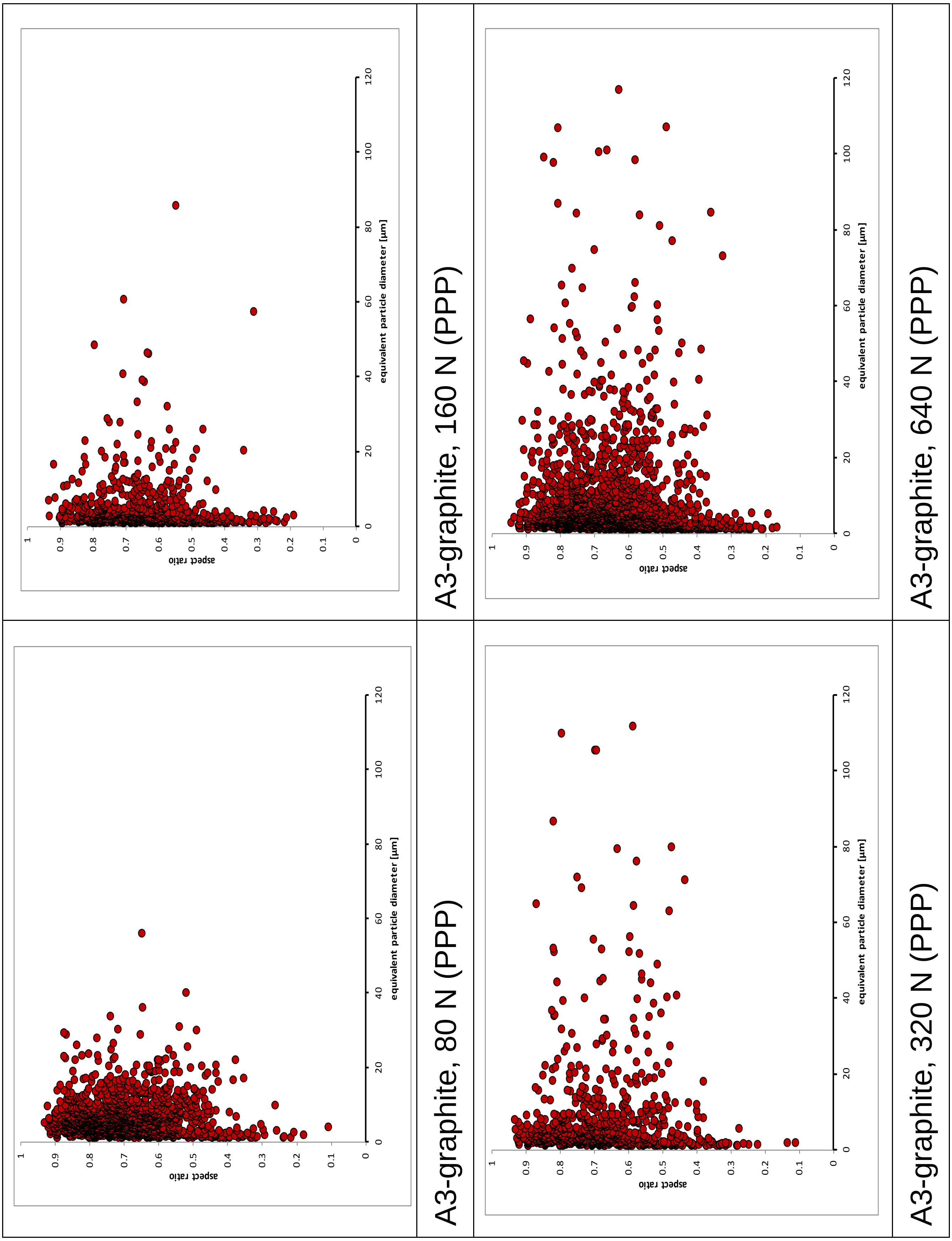

Figure 61: Comparison of aspect ratio (A3 pebble)

6.3 Comparison of the cumulative particle size distributions of particles obtained by friction of MLRF pebbles

Similarly to the results of A3 pebble friction, the number of relatively large particles obtained by MLRF pebble friction increases with increasing contact force while the particle size distribution widens. For all experiments, the number-weighted median diameter of the particle samples was observed to be below 4 µm. The area-weighted diameter increased significantly with increasing contact force, particularly due to the large particles (d_p>40 µm). The highest area-weighted diameter was obtained at a contact force of 320 N, even higher than the one obtained at 640 N. This may be due to mechanical destruction of particle agglomerates generated by pebble friction. While the number-weighted median particle diameter of MLRF pebble friction does not significantly deviate from that of A3 pebble friction, the MLRF area weighted median particle diameter is significantly below the one for A3 pebbles. The diagram for the different loads can be seen in figure 62.

6.4 Comparison of the aspect ratio of particles obtained by friction of MLRF pebbles

Within the measurement uncertainty, no significant deviation between aspect ratios of A3 and MLRF pebble graphite particles could be determined. As in the A3 case, the aspect ratio was between 0.3 and 0.9 for all particles with most particles exhibiting aspect ratios between 0.5 and 0.8. Figure 63 shows the comparison of the MLRF graphite particles aspect ratio for different loads.

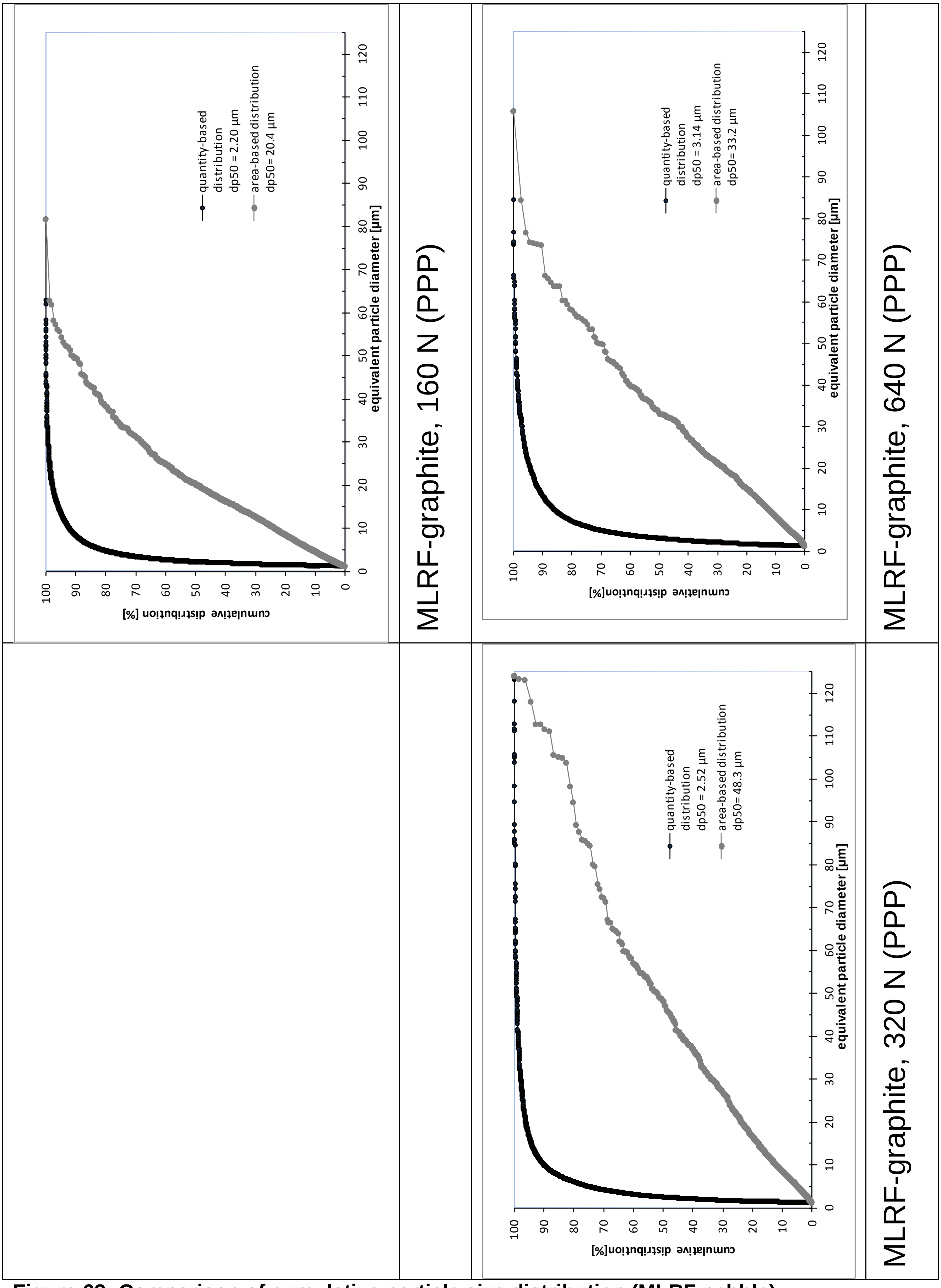

Figure 62: Comparison of cumulative particle size distribution (MLRF pebble)

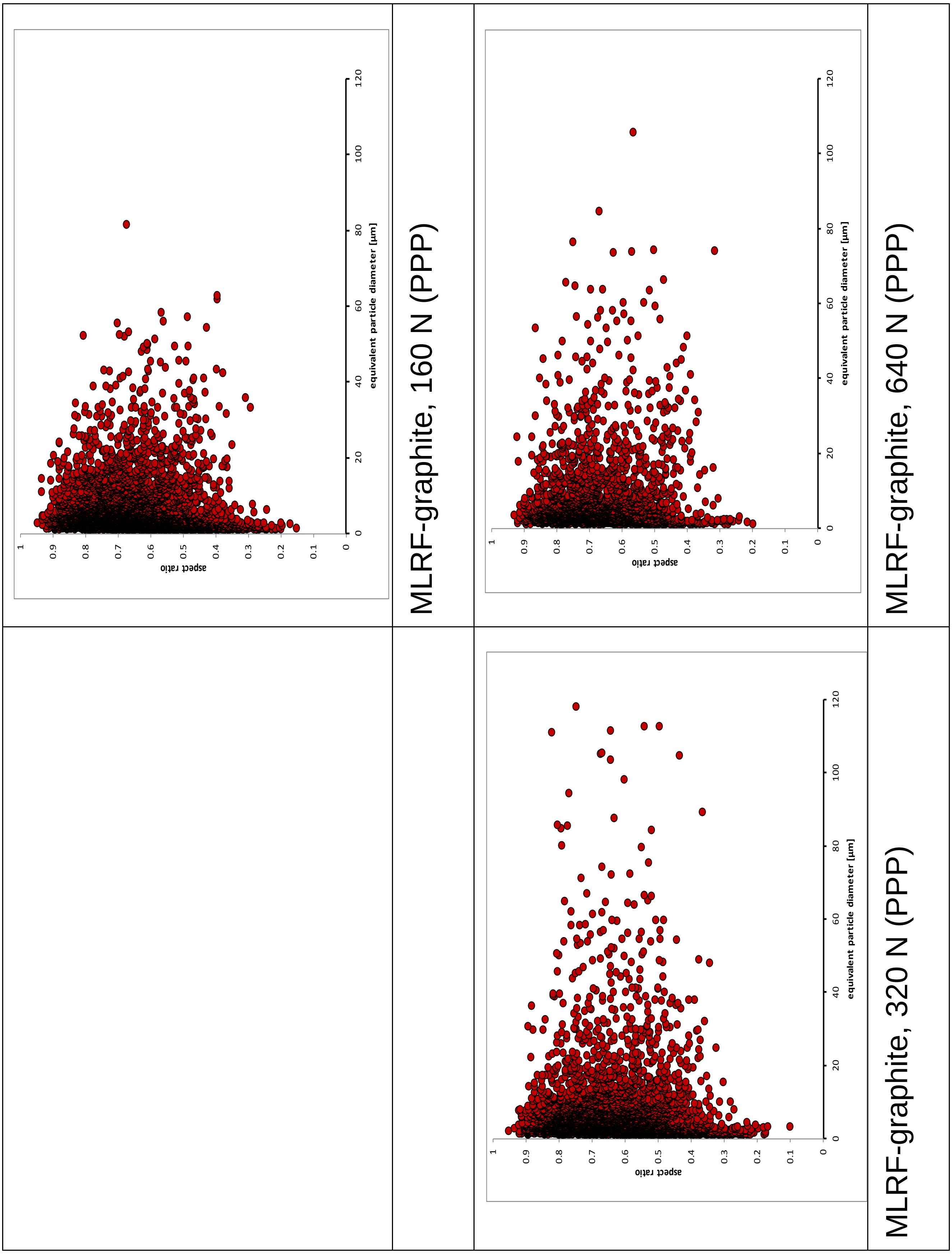

Figure 63: Comparison of aspect ratio (MLRF pebble)

7 Annexes

Annex 1 – Document approval by beneficiaries' internal QA

Annex 2 – Literature

7.1 Annex 1: Document approval by beneficiaries' internal QA

Fill involved beneficiaries as appropriate (mandatory for Milestones and Deliverables, but optional for other document type)

#	Name of beneficiary	Approved by	Function	Date
1				
2				
3				
4				
6				
7				
8				
9				
10				
11				
12				
13				
14				
15				
16				
17				
18				
19				
20				
21				

7.2 Annex 2: Literature

[1] **Ziermann, E., Ivens, G.**: *Abschlußbericht über den Leistungsbetrieb des AVR-Versuchskraftwerkes*, Report 3448, Forschungszentrum Jülich GmbH, 1997

[2] **Stempniewicz, M.M., Winters, L., Caspersson, S.A.:.** *Analysis of dust and fission products in a pebble bed NGNP*, Nuclear Engineering and Design 251 (2012), 433-442.

[3] **Schreier M.; Lustfeld M.; Lippmann W.; Hurtado A.:** *Graphite Dust Production by Friction with the Test Facility „Pebble Mill"***,** ARCHER Deliverable 23.22, TU Dresden, 2013

[4] **Burger W., Mark J.B.:** *Digitale Bildbearbeitung – Eine Einführung mit Java und ImageJ* (2.Auflage), Springer-Verlag, Hagenberg/ Washington D.C., 2006

[5] **Stieß M.:** *Mechanische Verfahrenstechnik – Partikeltechnologie 1 (3. Auflage)***,** Springer Verlag, Konstanz, 2008

[6] **Mandø, M., Rosendahl, L.:** *On the motion of non-spherical particles at high Reynolds number*, Powder Technol. 202 (2010),pp 1-13.

[7] **Deutsches Institut für Normung e. V.,** *Darstellung der Ergebnisse von Partikelgrößenanalysen - Teil 6: Deskriptive und quantitative Darstellung der Form und Morphologie von Partikeln (ISO 9276-6:2008),* Berlin: Beuth Verlag GmbH, 2012.

[8] **Schreier M.; Lustfeld M.; Lippmann W.; Hurtado A**.: *Report on Establishment of a small generic Test Facility (pebble mill)*, ARCHER Deliverable 23.21, TU Dresden, 2012